Recombinant expression of type IV pilins supports new model of pilus assembly

Justin Nathaniel Applegate

A dissertation

submitted in partial fulfillment of the

requirements for the degree of

Doctor of Philosophy

University of Washington

2026

Reading Committee:

Alexey J. Merz, Chair

Beth Traxler

Claudia Vasquez

Program Authorized to Offer Degree:

Department of Biochemistry

University of Washington

Abstract

Recombinant expression of type IV pilins supports new model of pilus assembly

Justin Nathaniel Applegate

Chair of the Supervisory Committee:

Professor Alexey J. Merz, PhD

Biochemistry

Type IV pili are essential virulence factors for many pathogenic bacteria including *Neisseria gonorrhoeae*. Their functions include: twitching motility, biofilm formation, DNA uptake, and host cell adhesion. Several proteins at the tip of the fiber – namely PilI, PilJ, PilK, and PilC – form an initiation complex that is essential to efficient pilus formation. The exact mechanism and configuration by which these proteins assemble into the fiber has previously been unknown. We have developed a new method for recombinant expression of type IV pilin proteins. By engineering a signal peptidase I sequence into the α-helical spine of the pilins, we are able to purify them from the periplasm without the use of detergents that could disrupt protein-protein interactions. Using this method we were able to identify an obligate heterodimer formed by PilI and PilJ. Additionally, we were able to detect PilK and the C terminal half of PilC forming a complex. These results combined with alphafold modeling and cell based assays

support a model where the extreme C terminus of PilC binds to PilK as the first step of pilus assembly. This PilC-PilK dimer is then able to bind to the PilI-PilJ dimer, forming the capping complex which primes pilus extension.

TABLE OF CONTENTS

TABLE OF FIGURES

TABLE OF TABLES

Acknowledgements:

Thank you Alex for being a great PI. Shortly after joining your lab, when I experienced a personal tragedy, you told me "Work hard when you can; take care of yourself when you should." That moment stuck with me. My time in grad school has been filled with highs and lows and I am grateful for your unending support throughout all of it.

I'd like to thank all of my other scientific mentors who guided me on my path. I am especially grateful for everyone I've met through the STI/HIV training grant, and Dana Miller, without whom I likely never would have found my way to Seattle.

Thank you to Emma, Zoey, Sena and every other member of the Merz Lab past and present for creating a lab that I am proud to be a part of every day. Thank you to the Seattle Mariners Star System coined by Emma Mackey for keeping me motivated each week for all these years. It is no exaggeration to say without those stickers on the line, this dissertation would never have been completed. Thank you to the Seattle Mariners themselves for teaching me how to carry on in the face of unending failure.

To Briar, Nesta, Jon, Marisa, Erin, Deidra, Tegan and every other loved one I've met in Seattle I am so grateful you are in my life.

Thank you to Blossom's Bloom, The Dry/Wet Peabos Collective, The Garages, Thank The Bus Driver, Cat Girl Homicide, Girl Only Consoles, and anyone else I've made music with in the past six years.

Thank you Landon for always being there to chat when I'm getting groceries or picking up photos. I am happier every day that you continue to be in my life.

Finally, Thank you to Mom, Dad, and Sarah for all the ways you've helped me become the person I am today.

Dedication:

To Nana and Poppy

Chapter 1. Introduction

Gonorrhea is a sexually transmitted infection caused by the gram-negative bacterium *Neisseria gonorrhoeae* (Ng). With over 500,000 cases of infection reported annually it is the second most common notifiable disease in the US, behind chlamydia (CDC 2025). This infection can lead to pelvic inflammatory disease, infertility, ectopic pregnancy, chronic pelvic pain, disseminated gonococcal infection, and endocarditis (Hill et al. 2016; Lenz and Dillard 2018). It is also thought to increase the efficiency of HIV transmission (Jarvis and Chang 2012). Ng is a close relative of the lethal pathogen *N. meningitidis*. In accordance with a recent Presidential Memorandum, the CDC has removed several vaccines from their recommendations for all children, including meningococcal ACWY, and meningococcal B (CDC 2026). This has potential to result in an increase in incidences of infection, making study of these organisms especially relevant.

For my thesis work, I sought out to understand one essential aspect of pathogenic *Neisseria* spp.: the type IV pilus and the initiation of its assembly. As I will describe in this chapter, type IV pili (T4P) are necessary for host cell adhesion, biofilm formation, twitching motility, and DNA uptake. They facilitate the spread of antimicrobial resistance genes, making them a pressing concern.

1.1 *Neisseria gonorrhoeae*: a historical overview

References to gonorrhea can be found in texts dating back to as early as 2600 BCE (Lee and Ladizinski 2012). Throughout history there have been many attempts to treat “the perilous infirmity of burning” (Sanger 1910). Historical treatments have included mercury injections, bloodletting, heat therapy, and silver nitrate, each with varying results (Jose et al. 2020). This

changed in 1937, with the introduction of sulfonamides for the treatment of gonorrhea (Dees and Colston 1937).

The use of antibiotics had proven to be a quick and effective treatment. However, by the 1940's, sulfonamide treatment had a nearly 30% failure rate for gonorrhea treatment due to a rise of drug resistance. This prompted the use of penicillin as treatment, which was followed by a rise in penicillin resistance (Herrell et al. 1943). This pattern has continued to the present. Since 1937, several classes of antimicrobials have been introduced as treatment for gonorrhea, including: sulfonamides, penicillins, aminocyclitols, tetracyclines, fluoroquinolones, macrolides, and cephalosporins. Each has been followed by the emergence of resistance (Unemo et al. 2019). Ng is naturally competent for DNA transformation, and can obtain alleles encoding antibiotic resistance *via* horizontal gene transfer. Competence requires the type IV pilus, the structure at the center of this dissertation. Ng may also acquire resistance alleles through conjugal transfer from other organisms (Fiore et al. 2020).

Today, the cephalosporin ceftriaxone is recommended by the WHO and CDC as standard care for uncomplicated gonococcal infection (World Health Organization 2024; CDC 2025). Cases of ceftriaxone-resistant Ng have been observed clinically (Day et al. 2022). Concerns over antimicrobial resistance informed the CDC doubling the recommended dosage from 250 mg to 500 mg in 2020 (Sancta St. Cyr et al. 2020). The rising threat of multidrug-resistance in Ng underscores the need for alternative treatments such as vaccines.

There have been attempts to design a gonococcal vaccine since even before the use of antibiotics (Eyre and Stewart 1909). However, over the past century none have had clinical success (McChesney et al. 1982; Boslego et al. 1991; Jefferson et al. 2021). A recent breakthrough has renewed hope for an Ng vaccine. The 4CMenB vaccine, a serogroup B

meningococcal outer membrane vesicle-based vaccine, was found to provide cross-species protection against Ng (Leduc et al. 2020; Marshall et al. 2022). This protective effect has been shown to only be about ~35% effective in clinical trials, meaning the work toward a vaccine against Ng is promising but ongoing (Noori Goodarzi and Pourmand 2026).

There are many factors that make development of a vaccine difficult. Natural Ng infection does not protect against repeated reinfection. Additionally, humans are the exclusive reservoir of Ng. Because of this, many species specific interactions important to pathogenesis cannot be recapitulated in nonprimate organisms, or even in primates of the *Macaca* genus. Several surface exposed virulence factors – such as the type IV pilus – can undergo phase and antigenic variation, protecting from immune recognition (Stern et al. 1986; Seifert et al. 1994; Schmidt et al. 2001).

Type IV pili are essential to Ng's ability to cause infection in humans. Clinical strains are consistently piliated, and non-piliated mutants are unable to cause disease or infection in human challenge studies (Kellogg et al. 1963; Hobbs et al. 2011). Pili facilitate initial adhesion to the host cells, aid in immune evasion, protect against oxidation, and mediate the spread of antimicrobial resistance genes (Punsalang and Sawyer 1973; Quillin and Seifert 2018; Hu et al. 2022). For these reasons the study of T4P is especially relevant to understanding gonococcal pathogenesis.

1.2 Type IV Pili

Type IV Pili (T4P) are dynamic, proteinaceous fibers that are present in many Gram negative bacteria including known pathogens including *Vibrio cholerae*, *Haemophilus influenzae*, *Pseudomonas aeruginosa*, and *Legionella pneumophila* (Berry and Pelicic 2015).

They can also be found in Gram positive bacteria including *Streptococcus* Spp. and Archaea, suggesting that T4P were present in the last universal common ancestor of life (Makarova et al. 2016). T4P are able to facilitate cell movement through twitching motility, biofilm formation and colony dynamics, and also mediate DNA uptake, phage infection, and host cell adhesion (A. J. Merz et al. 2000; Welker et al. 2018; C. K. Ellison et al. 2018; Quillin and Seifert 2018).

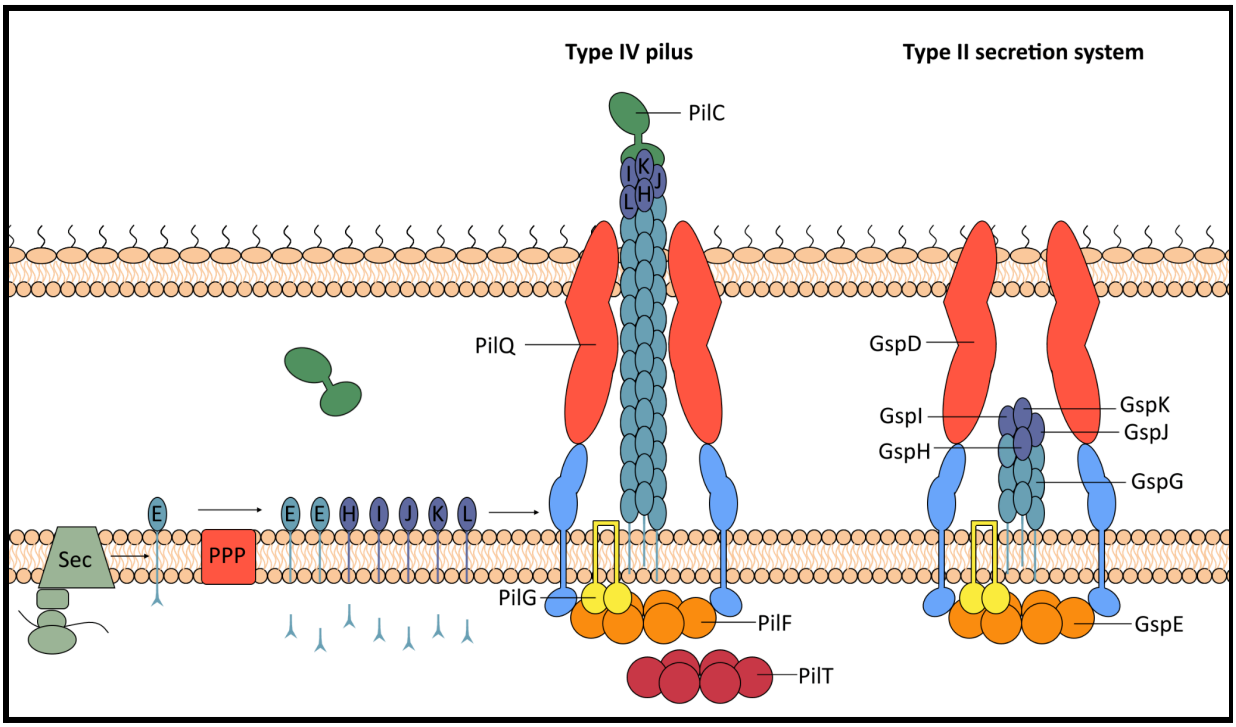

Figure 1-1. Structure and Assembly of Type IV Fiber Systems
Pilin (PilE) and minor pilin (PilH-L) molecules enter the bacterial inner membrane as prepilins before processing by prepilin peptidase (PPP). The minor pilins and PilC prime extension of the fiber. The fiber extends out of the outer membrane secretin channel (PilQ) which is bound to the inner membrane machinery by alignment proteins (PilM-P). Cytosolic ATPases (PilF and PilT) drive pilus assembly and disassembly via conformational changes transduced by the platform protein (PilG). Tfp machinery is homologous to type II secretion system machinery.

T4P fibers are 6 nm in diameter, span the periplasm and can extend up to several μm (Craig et al. 2006). There are several key components required for pilus assembly in Ng (Figure 1-1). Two cytosolic AAA family ATPase motors, PilB and PilT, power pilus extension and retraction. PilT can drive retraction with forces exceeding 100 pN (A. J. Merz et al. 2000; Maier

et al. 2002). PilG is hypothesized to act as a transmembrane platform protein which transfers the force generated by the cytosolic motor proteins into the periplasm for fiber assembly. PilQ forms a pore in the outer membrane for the fiber to extend out of, and PilM, PilN, PilO, and PilP help to align PilQ with the inner membrane proteins (Craig et al. 2019).

The T4P fiber is assembled from a pool of integral cytoplasmic membrane protein subunits called pilins. The major pilin subunit PilE is made of a C-terminal α-helical spine that is incorporated into the inner membrane, and a N-terminal globular head domain which faces the surface of the assembled fiber. Pilin proteins translocate into the cytoplasmic membrane and periplasm via the SecYEG pathway, and are processed by the prepilin peptidase PilD. PilD is a bifunctional enzyme that first cleaves the N-terminal cytoplasmic tail of the pilin, then N-methylates it (Nunn and Lory 1991; Francetic et al. 2007).

Beyond PilE, there are several minor pilins which resemble the major pilin but are incorporated at lower quantities into the fiber. These minor pilins serve several functions. ComP is a DNA binding pilin which supports pilus mediated uptake of DNA containing a recognized DNA uptake sequence. PilV is reported to be involved in host cell interaction and inhibition of ComP. Either ComP or PilV must be expressed, or fiber assembly fails to occur (H. C. Winther-Larsen et al. 2001; Aas et al. 2002; Barnier et al. 2021). There are several minor pilins – PilH, PilI, PilJ, PilK, and PilL – expressed from a polycistronic mRNA. Each of these is essential for efficient pilus assembly, and all are believed to be localized to the tip of the fiber (Hanne C. Winther-Larsen et al. 2005).

At the very tip of the T4P of Ng is a 110 kDa adhesion protein, PilC. The Ng chromosome contains two copies of the *pilC* genes, translationally controlled by a frameshift mutation in the polyG tract preceding them. Switching between the translated and non-translated

states is called phase variation. Expression of at least one PilC protein is required for piliation (Jonsson et al. 1991). Individual subunits are added to the base of an assembling T4P fiber, meaning that the proteins at the tip are the first to be assembled. The type II secretion system (T2SS) is homologous to T4P but lacks an adhesive payload like PilC. A structure of the T2SS capping complex, made of the minor pilin homologs GspI, GspJ, and GspK, has been solved (Korotkov and Hol 2008; Yanez et al. 2008; Korotkov et al. 2012). The minor pilins and PilC have proven to be more difficult to study with than T2SS pseudopilins, due in part to all of them containing disulfide bonds. While it had been known that the minor pilins and PilC form a capping complex which primes pilus extension, the structure of the minor pilins and how they associate had remained a mystery (Hanne C. Winther-Larsen et al. 2005; Nguyen et al. 2015; Treuner-Lange et al. 2020; Guo et al. 2024).

In Chapter 2, I outline a method for recombinant expression of these minor pilins while maintaining protein-protein interactions. This method has allowed the isolation of a subcomplex made of PilI and PilJ. In Chapter 3, this method is applied and combined with *in silico* modeling, bioinformatic analysis and cell based assays to investigate the assembly of the initiation complex, and how it primes pilus biogenesis.

Chapter 2. Expression of soluble Type IV Minor Pilins and isolation of a Neisseria gonorrhoeae PilI-PilJ subcomplex

Chapter 2 is adapted with minimal modification from:

Expression of soluble Type IV Minor Pilins and isolation of a Neisseria gonorrhoeae PilI-PilJ subcomplex

Justin Applegate, Emma Miller, Zoey Litt, Afredo Ruiz-Rivera, Angela Lisovsky, Beth Traxler, Alexey Merz

bioRxiv 2026.02.09.704877; doi: https://doi.org/10.64898/2026.02.09.704877

2.1 Abstract

Type IV pili and type II secretion systems assemble dynamic fibers used by bacteria and archaea for diverse functions. The pilus fiber is made up of major and minor pilin subunits containing a hydrophobic α-helical spine and a globular head. Purifying minor pilins is complicated by the hydrophobic α-helical spine, frequently present disulfide bonds, and low abundance within the fiber. These challenges have impeded structural and functional studies of pilin protomers. Here, we describe a method for expression and purification of soluble type IV pilin proteins from *Escherichia coli*. Signal peptidase I cleavage sites are engineered into the α-helix of the pilin proteins. This allows their globular domains to be purified from the periplasmic fraction. We used this method to obtain the Neisseria gonorrhoeae minor pilins PilI and PilK in soluble form. In a third case, where the minor pilin PilJ could not be obtained on its own, coexpression with PilI and purification of a PilI-PilJ heterodimer was possible. We suggest that PilI and PilJ form an obligate heterodimer that is essential for their function.

2.2 Importance

Type IV pili are essential to many bacteria responsible for disease. They can be found in both Gram-negative and Gram-positive bacteria, as well as archaea, making them likely present in the last common ancestor of all life on Earth. Despite their significance in a variety of species, there are large gaps in our understanding of the structure of these diverse biological machines. One roadblock to this research has been the difficulty of purifying the minor pilin proteins that serve different functions in the fiber. Here, we describe a novel method for the purification of these proteins and demonstrate the ability of this method to identify a protein-protein interaction between two minor pilins of *Neisseria gonorrhoeae*.

2.3 Introduction

Type IV pili (T4P) are found in diverse organisms including Gram-negative and Gram-positive bacteria, as well as archaea. They were likely present in the last common ancestor of all life on Earth (Makarova et al. 2016). These protein fibers are used in twitching motility, surface sensing, biofilm formation, DNA uptake, and adhesion to host cells (Craig et al. 2019; Singh et al. 2022). T4P are essential virulence factors for many pathogenic organisms including *Neisseria gonorrhoeae*, the etiologic agent of gonorrhea. The pilus fiber is composed of pilin subunits, which include the major pilin that makes up most of the fiber, and minor pilins, which structurally resemble the major pilin but are present in the fiber in lower proportions. These minor pilins can serve several functions. In *N. gonorrhoeae,* PilV and ComP are involved in host cell adhesion and DNA uptake (Hughes-Games et al. 2022), while other pilins including PilI, PilJ, and PilK are essential for efficient pilus formation (Hanne C. Winther-Larsen et al. 2005).

Both major and minor prepilins consist of an N-terminal pilin signal sequence, a hydrophobic α-helical domain and a C-terminal globular head domain. The cytoplasmic N-terminal portion of the prepilin signal sequence is cleaved by a bifunctional enzyme, prepilin peptidase. Mature pilins are then N-methylated by the same enzyme (Nunn and Lory 1991). We follow the convention of numbering pilin amino acids from the first residue of the cleaved, mature pilin. The α-helical spines of pilins are embedded within the inner membrane, until the pilins are assembled into the fiber by the pilus assembly machine. T4P can also retract, depolymerizing from the base and releasing pilin protomers back into the cytoplasmic membrane pool. When an excessive quantity of pilin is present in the membrane and fiber assembly is disrupted, mature major pilins can be cleaved at the 39/40 residue, creating a soluble form of the globular domain, known as S-pilin. The protease responsible for this cleavage has not been identified (Giltner et al. 2012; Haas et al. 1987). It is not known whether S-pilin forms of the minor pilin proteins can occur.

Major pilin proteins have been purified in quantity from native fibers using mechanical shearing, followed by cycles of fiber precipitation. Pilin monomers or dimers are then obtained by dissolving the fibers in detergent, and major pilins can be further purified using ion exchange and size exclusion chromatography (Brinton et al. 1978; Parge et al. 1990; Gonzalez Rivera and Forest 2017). Purifying minor pilins through this approach is impractical, as there are only small numbers of minor pilin molecules per fiber. In the case of tip-located minor pilins, there is likely only one molecule per fiber.

Any purification approach must consider the pilin protomer's hydrophobic transmembrane α-helical spine. Moreover — and in contrast to the related pilins of type II secretion systems — most type IV pilins contain one or more disulfide bonds, which form only

after translocation of the globular domain across the cytoplasmic membrane into the periplasm (or, in Gram positive bacteria and Archaea, the extracellular compartment). Recombinant purification is a useful strategy for obtaining larger quantities of pilin proteins. The full-length major pilin of *Acidithiobacillus thiooxidans* was purified from *Escherichia coli* using a thioredoxin fusion and detergents to maintain solubility (Páez-Pérez et al. 2025). For biochemical and structural applications, it is valuable to have forms of minor pilin proteins that remain soluble in the absence of lipids or detergents. For this purpose, truncated pilin globular domains are often expressed. Some soluble domains of pilins have been recombinantly expressed in the cytoplasm of engineered *E. coli* cells with aberrant redox potential (Karuppiah et al. 2016; Craig et al. 2003). To allow truncated pilins to fold in the periplasm, they have at times been expressed as fusions to a periplasmic protein like maltose-binding protein (Helaine et al. 2007), or bearing signal sequences from periplasmic proteins such as OmpA (Hazes et al. 2000) or DsbA (Ramboarina et al. 2004). The type II secretion system (T2SS) is closely related to the type IV pilus. Structural data for T2SS minor pseudopilins, homologous to the minor pilins of T4P, was obtained by expressing the globular domains cytosolically in *E. coli*. In some cases this required refolding from inclusion bodies and years of effort (Korotkov and Hol 2008; Yanez et al. 2008; Korotkov et al. 2012). In contrast to T2SS pseudopilins, most T4P minor pilins have one, two, or more disulfide bonds, making these targets even more challenging than T2SS pseudopilins.

To probe the assembly pathway of a Type II secretion pseudopilin, Francetic et al. (2007) introduced a signal peptidase I (SPI) cleavage site that would allow processing if the pseudopilin was translocated into the periplasm. They observed a soluble form of the globular domain, similar to naturally occurring major S-pilins in the T4P system. We took inspiration from this

approach to express and purify soluble T4P minor pilins from the *E. coli* periplasm. This method allows the proteins to fold as integral membrane proteins with oxidized disulfide bonds in the periplasm. Soluble globular pilins can then be recovered from the periplasmic space without the use of detergents that could interrupt protein-protein interactions or interfere with downstream assays.

2.4 Materials and Methods

2.4.1 Media and Buffers

LB medium contained 10 g/L Bacto Tryptone, 5 g/L Bacto Yeast Extract, 5 g/L NaCl, 1 mM NaOH. ZYM-5052 was prepared as described (Studier 2005). Sucrose Shock Buffer contained 0.1 M Tris-acetate at pH 7.8, 20% (m/v) sucrose, and 1 mM EDTA. 0.5 mM $MgSO_4$ was used for osmotic shock. 10x PBS stock was prepared with 80 g/L of NaCl, 2.0 g/L KCl, 14.4 g/L Na_2HPO_4, 2.4 g/L KH_2PO_4. PBST contained 1x PBS with 0.1% Tween-20. Wash Buffer A contained 1x PBS + 10 mM imidazole, pH 7.8. Wash Buffer B contained 1x PBS + 350 mM NaCl + 10mM imidazole, pH 7.8. SDS-PAGE buffer contained 25 mM Tris Base, 192 mM Glycine, 0.1% SDS . 4X Laemmli buffer contained 0.250 M Tris base, 8% SDS, 40% glycerol, 20% 2-mercapto-ethanol, and Bromophenol blue.

2.4.2 Reagents

Most chemicals were obtained from Sigma-Aldrich. Phenylmethylsulfonyl fluoride was from Fisher Scientific (P/2805/44) and Ni-Sepharose High Performance resin was from Cytiva (#17526802).

2.4.3 Design of cleavage sites

N. gonorrhoeae minor pilin sequences were redesigned to contain a Signal Peptidase I cleavage site within the α-helical region (typically around residue +25, where the first residue of the processed, mature full-length pilin in a native context is defined as +1). SignalP v. 5.0 (Almagro Armenteros et al. 2019) was used to predict the ability of these sites to be recognized. Sequences were altered until SignalP v. 5.0 gave a probability over 0.6. We found that a more recent, machine learning-based release of SignalP (v. 6.0) (Teufel et al. 2022) was not suitable for this purpose, because it dominantly recognizes native prepilin peptidase processing sites in pilin signal sequences, rather than the introduced SPI cleavage sites. (Note that prepilin peptidases are not present in the *E. coli* hosts that we employ for expression.) Predictive structural modeling of the engineered minor pilins was performed using Alphafold2 *via* CollabFold (Mirdita et al. 2022), or Alphafold3 *via* Google Alphafold Server (Abramson et al. 2024).

2.4.4 Cloning

Expression vectors were prepared with standard methods. In brief, a geneblock (IDT, Inc.) was designed to encode the designed minor pilin with an introduced SPI cleavage site and a C-terminal TEV-His_6 tag. These sequences were amplified by PCR and inserted into the pET22B-derived plasmid pHIS-Parallel1 (Sheffield et al. 1999) between the NdeI and NcoI cut sites, by the method of (Gibson et al. 2009). For the bicistronic vector containing *pilI* + $pilJ_{short}$, the open reading frames were inserted between NdeI and BlgI. Sequences for all expression vectors used are presented in the Supplemental Materials outlined in Table 2-S1.

2.4.5 Culture growth and expression conditions

Expression vectors were transformed into competent *E. coli* BL21(DE3) cells. A single colony was picked and added to LB medium supplemented with 100 ug/ml ampicillin. This culture was grown overnight shaking at 200 rpm at 37° C. 5 mL of seed culture was added to a 2 L baffled flask containing 1 L ZYM-5052 (Studier 2005), supplemented with 100 µg/ml ampicillin, then grown at 37° C, shaking at 200 rpm. When cells reached an optical density at 600 nm of 1.0, they were moved to a 16° C incubator and shaken at 200 rpm. Cultures were grown for an additional 18 hours before being harvested by centrifuging at 4670 x g for 15 min and 4° C (Sorvall H6000A, RC-3B Refrigerated Centrifuge).

2.4.6 Isolation of Periplasmic Fraction

Immediately after centrifugation, pelleted cells were chilled on ice for 10 minutes then gently resuspended in 10 mL of ice cold sucrose shock buffer per 10 g of cell pellet. The cell suspension was chilled on ice for 10 minutes before being centrifuged at 4670 x g for 15 min and 4° C (Sorvall H6000A, RC-3B Refrigerated Centrifuge). The supernatant was collected. To the collected supernatant, 10x PBS was added to a final concentration of 1x, and 200 mM phenylmethylsulfonyl fluoride (PMSF) was added from a 2-propanol stock to a final concentration of 1 mM. The pelleted cells were chilled on ice for 10 minutes then gently resuspended in 5 mL of ice-cold 0.5 mM $MgSO_4$ per 10 g of cells. The cells were incubated on ice for 10 minutes in $MgSO_4$ then centrifuged at 4670 x g for 15 minutes and 4 °C (Sorvall

H6000A, RC-3B Refrigerated Centrifuge). The supernatant was collected. 10x PBS was added to a final concentration of 1x and 200 mM PMSF was added to a final concentration of 1 mM.

2.4.6 Immobilized metal affinity purification

Supernatants from both the sucrose shock and 0.5 mM $MgSO_4$ steps contained soluble minor pilins, so these fractions were pooled. For every 10 mL of pooled supernatant, 50 µL of packed Ni^{2+}-NTA sepharose HP (Cytiva) was equilibrated in 1X PBS. Equilibrated resin was added to the pooled supernatant and bound in batch, nutating for 1 hr on ice. Samples were then centrifuged for 8 minutes at 500 x g and 4° C (TX-400 rotor, Sorvall Legend X1R). Supernatant was removed and resin was washed 3 times, with resuspension in wash buffer and centrifugation as in the previous step. For the first wash, the resin was resuspended in 5 mL of Wash Buffer A. For the second wash, the resin was resuspended in 10 mL of Wash Buffer B. For the third wash, the resin was resuspended in 5 mL Wash Buffer A. After washing the resin slurry was transferred to a chilled column. Bound material was eluted from the column using elution buffer (PBS + 350 mM imidazole), collected in 0.5 mL fractions.

2.4.7 SDS-PAGE and immuno-blotting

Samples were mixed with 4x Laemmli buffer containing 20% 2-mercapto-ethanol (5% v/v final) then incubated at 95° C for 5 minutes. Samples were loaded into 12.5% (w/v) SDS-PAGE gels and run for 60 minutes at 190 V. Gels were either stained with Coomassie blue or for immuno blotting transferred to a 0.45 µm nitrocellulose membrane (Schleicher & Schuell BA85). Membranes were blocked with PBS Blocking Buffer (LICORbio) for 1 hr at room

temperature then incubated with primary antibody (His.H8, Invitrogen MA1-21315) for 1 hour at room temperature. The membrane was rinsed in PBST 5 times for 5 minutes before being incubated with secondary antibody diluted 1:10,000 (Goat anti-Mouse IgG H+L Highly Cross-Adsorbed Secondary Antibody Alexa Fluor 488, Invitrogen A32723TR) for 45 minutes at RT. Membrane was then rinsed in PBST 5 times for 5 minutes and imaged using an Odyssey imaging system (LI-COR Biotech).

2.5 Results and Discussion

2.5.1 Design of SP1-celavable pilins

Type IV pilins are substrates of the PilD prepilin peptidase, which cleaves at the cytoplasmic face of the plasma membrane. Pilins do not natively contain SPI signal sequences, which are cleaved at the periplasmic face of the plasma membrane. SPI sequences are defined by a positively charged N-terminal region, a central hydrophobic region, a helix-breaking residue at position -4 to -6 relative to the cleavage site, and compact amino acid residues at positions -1 and -3 (Kaushik et al. 2022). The minor pilin PilK from *N. gonorrhoeae* strain MS11A was engineered to introduce a SPI cleavage site within its α-helical spine. This was accomplished by iterative cycles of *in silico* mutagenesis and signal sequence prediction, using the SignalP v. 5.0 algorithm (Almagro Armenteros et al. 2019). In PilK, we replaced the region from T37 to Y42 (TAAQSY) with PGAQASD (Figure 2-1B). SignalP v. 5.0 predicted a SPI cleavage site between A41 and S42 with a probability of 0.647. By contrast, in wild type PilK, the SPI cleavage probability was predicted to be 0.064 (Supplementary Figure 2-S1).

A

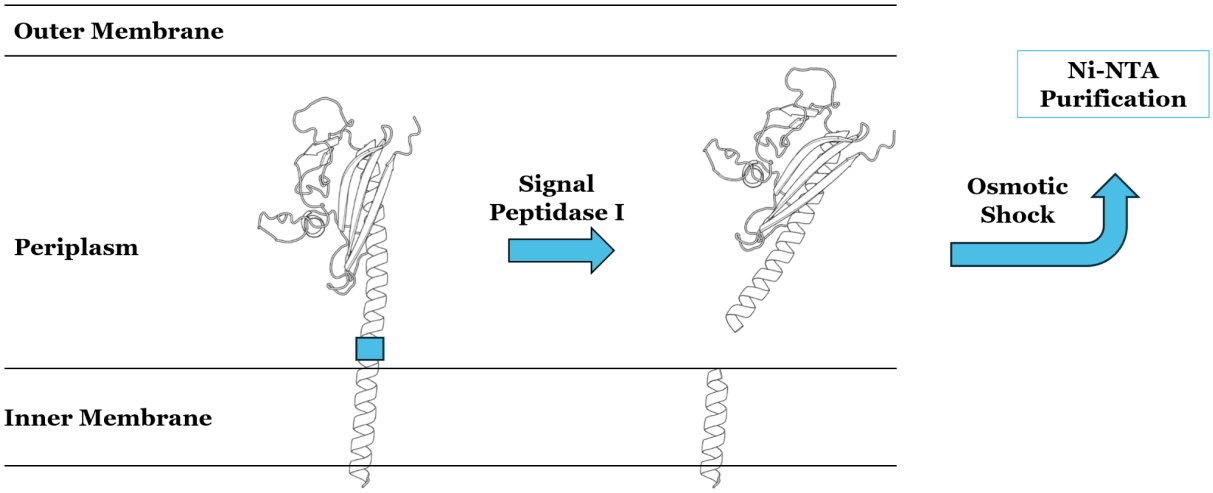

B

```
PilK WT-          MRKQNTLTGIPTSDGQRGSALFIVLMVMIVVAFLVVTAAQ-SYNTEQRISANESDRKLALSLAEAALR…
PilK SPI-         MRKQNTLTGIPTSDGQRGSALFIVLMVMIVVAFLVVPGAQASDNTEQRISANESDRKLALSLAEAALR…

PilI WT-          MKNNDCLRLKNPQSGMALIEVLVAMLVLTIGILALLSVQLRTVASVREAETQTIVSQITQNLMEGMLI…
PilI SPI-         MKNNDCLRLKNPQSGMALIEVLVAMLVLTIGILALLPGAQAS-------ETQTIVSQITQNLMEGMLI…

PilJ WT-          MKRKMLNVPKGGYDGMKGFTIVEFLVAGLLSVIVLI---AVVSSYFTSRKLNDAANERLAEQQDLRNA…
PilJ SPI-         MKRKMLNVPKGGYDGMKGFTIVEFLVAGLLSVIVLIPGAQASETYFTSRKLNDAANERLAEQQDLRNA…
PilJshort SPI-    MKRKMLNVPKGGYDGMKGFTIVEFLVAGLLSVIVLIPGAQADEN--------------LAEQQDLRNA…
```

Figure 2-1 Signal Peptidase I cleavage of engineered minor pilins
A. A model for the post translational processing of pilins is shown. Signal Peptidase I cuts at an engineered SPI cut site. **B.** N-terminal sequences of minor pilins containing engineered Signal Peptidase I (SPI) are shown. Residues that diverge from the wild type are in blue. Red arrowheads indicate the engineered cleavage sites.

A plasmid was prepared to express the putatively cleavable variant of PilK in *E. coli*. Cultures were grown, expression was autoinduced, and a periplasmic fraction was isolated. In anti-His_6 immunoblots, the whole-cell lysate contained two labeled species corresponding to the predicted masses of full-length and SPI-cleaved PilK-His_6. In contrast, the soluble periplasmic

fraction contained only the faster-migrating species, corresponding to SPI-cleaved, truncated PilK-His_6 (Figure 2-2B). This indicates that the minor pilin is expressed and that the globular domain is processed at the engineered SPI cut site. Following immobilized metal chromatography, the soluble PilK-His_6 fragment had a high yield of up to 20 mg of protein per L of starting culture (Figure 2-2A).

Putatively cleavable variants of PilI and PilJ were also designed (Figure 2-1B). For the engineered PilI-His_6, SignalP5.0 predicted the likelihood of SPI cleavage to be 0.675, and for PilJ-His_6, 0.565. PilI expressed well, with a yield of approximately 16 mg per L of culture (Figure 2-2D). Although a variety of growth and induction conditions were tested, we were unable to purify PilJ-His_6 using the initial design (Figure 2-3A).

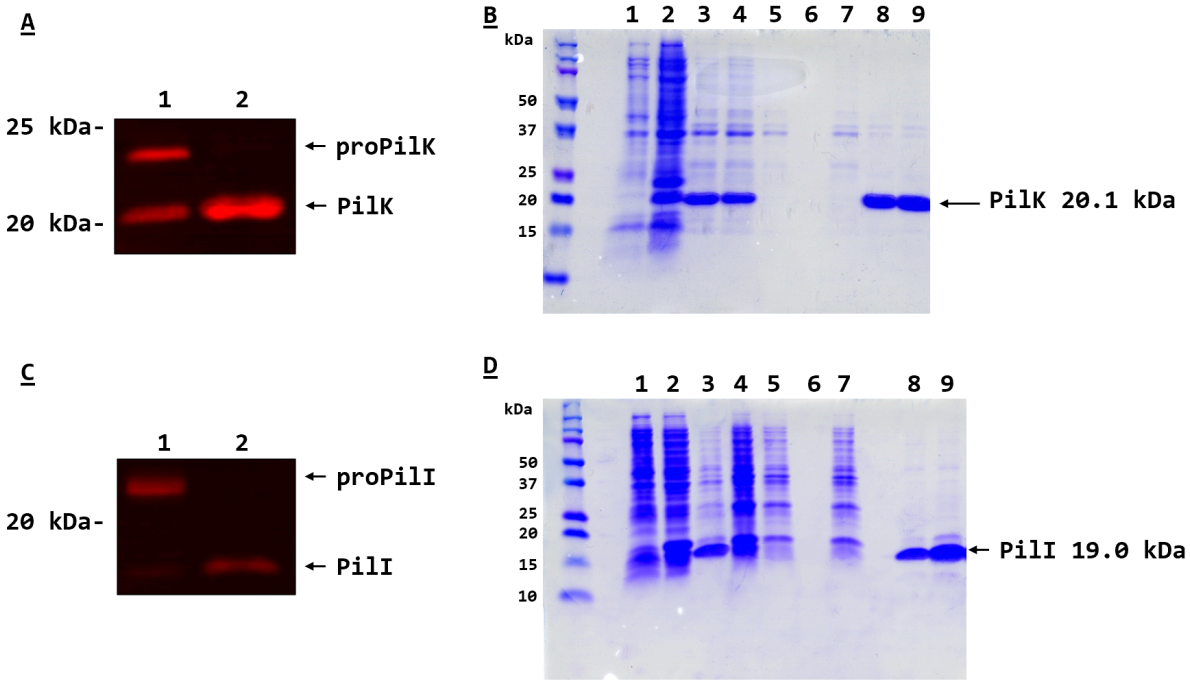

Figure 2-2 Introduced SPI sites yield soluble minor pilin fragments.

- **A.** Expression of engineered soluble minor pilin PilK-His_6 was analyzed by anti-His_6 immunoblot. Lane 1: whole cell lysate. Lane 2: periplasmic fraction.
- **B.** Purification of PilK-His_6. Lane 1: pre-induction cell lysate. Lane 2: post-induction cell lysate. Lane 3: sucrose shock supernatant. Lane 4: $MgSO_4$ supernatant. Lane 5: $MgSO_4$ fraction affinity resin flowthrough. Lane 6: $MgSO_4$ final wash. Lane 7: sucrose shock affinity resin flowthrough flowthrough. Lanes 8 and 9: eluted soluble PilK-His_6.
- **C.** Expression of engineered minor pilin PilI-His_6 was analyzed by anti-His_6 immunoblot. Lane 1: whole cell lysate. Lane 2: periplasmic fraction.
- **D.** Purification of PilI-His_6. Lane 1: pre-induction cell lysate. Lane 2: post-induction cell lysate. Lane 3: sucrose shock supernatant. Lane 4: $MgSO_4$ supernatant. Lane 5: $MgSO_4$ affinity matrix flowthrough. Lane 6: final affinity resin wash. Lane 7: sucrose shock affinity matrix flowthrough. Lanes 8 and 9: eluted soluble PilI-His_6.

To understand why the engineered PilJ-His_6 may have expression issues, we used Alphafold3 to predict its structure. We found that compared to the minor pilins that expressed well, this design of PilJ had a larger hydrophobic region on the C-terminal side the SPI cleavage site. The cleavage site could not be moved downstream without interfering with its ability to be cut. Thus, another construct for PilJ expression, $PilJ_{short}$-His_6, was constructed, lacking 14 residues downstream of the cleavage site (Figure 2-1B). SignalP v. 5.0 predicted the likelihood of $PilJ_{short}$-His_6 SPI cleavage to be 0.582. Although $PilJ_{short}$-His_6 was expressed, we were still unable to purify it in soluble form.

2.5.2 Purification of a stable PilI-PilJ subcomplex

In a previous study, deletion of the *pilJ* gene in *N. gonorrhoeae* resulted in decreased PilI expression at steady state. Moreover, deletion of the *pilI* gene in *N. gonorrhoeae* resulted in almost undetectable PilJ expression (Hanne C. Winther-Larsen et al. 2005). These results

suggested the hypothesis that PilI and PilJ form a binary complex that stabilizes both proteins. In TIIS systems, the nearest paralogs of *N. gonorrhoeae* PilI and PilJ are Gsp/Eps I and J. Crystal structures of TIIS pseudopilins from *Vibro vulnificus* and enterotoxigenic *E. coli* revealed I-J dimers with extensive binding interfaces (Yanez et al. 2008; Korotkov and Hol 2008; A. Y. Lam et al. 2009). Similarly, our Alphafold3 modeling of PilI-PilJ predicted with high confidence that PilI and PilJ form a stable heterodimer with the monomers in the same general arrangement as in the TIIS crystal structures (Figure 2-3B). Based on this, a bicistronic vector co-expressing both PilI and $PilJ_{short}$ was prepared. Expression from this vector allowed for the purification of a heterodimer of $PilJ_{short}$-His_6 and PilI (Figure 2-3D). When run on an anti-His_6 immunoblot, both whole cell lysate and periplasmic fractions contained only a single $PilJ_{short}$-His_6 band, with a mass of approximately 30 kDa, the size of the predicted soluble cleavage product (Figure 2-3E). A band corresponding to the uncleaved precursor was not detected. This may indicate that the SPI site is processed more efficiently than those of engineered PilK or PilI alone.

Our findings strongly support the idea that PilI association stabilizes PilJ, and suggests that the *Neisseria* T4P tip complex and TIIS pseudopili share a conserved quaternary subunit structure. In a companion study (See Chapter 3), we present evidence that the N. gonorrhoeae PilI-PilJ heterodimer has a 1:1 stoichiometry, and that it functions as a recognition module for PilK and the tip adhesin PilC. In a working model, the PilI-PilJ module monitors formation of a complex between PilK and ~10 residues at the extreme C-terminus of the tip-located adhesin PilC. The resulting Pil I-J-K-C heterotetramer would then license polymerization of the helical T4P fiber through a templating mechanism. Purification of minor pilins is essential for studying type IV pili. Recombinant expression from *E. coli* has been useful but has posed a variety of technical challenges. The complementary approach outlined here allows for expression and

purification of these minor pilins in good yields, without the use of detergents that could interfere with protein-protein interactions. As we have seen with PilJ, interactions of these proteins can be essential to their stability and function. Further structural and biophysical characterization of minor pilin interactions is needed to understand the assembly, dynamics, and functions of type IV pili and type II secretion systems.

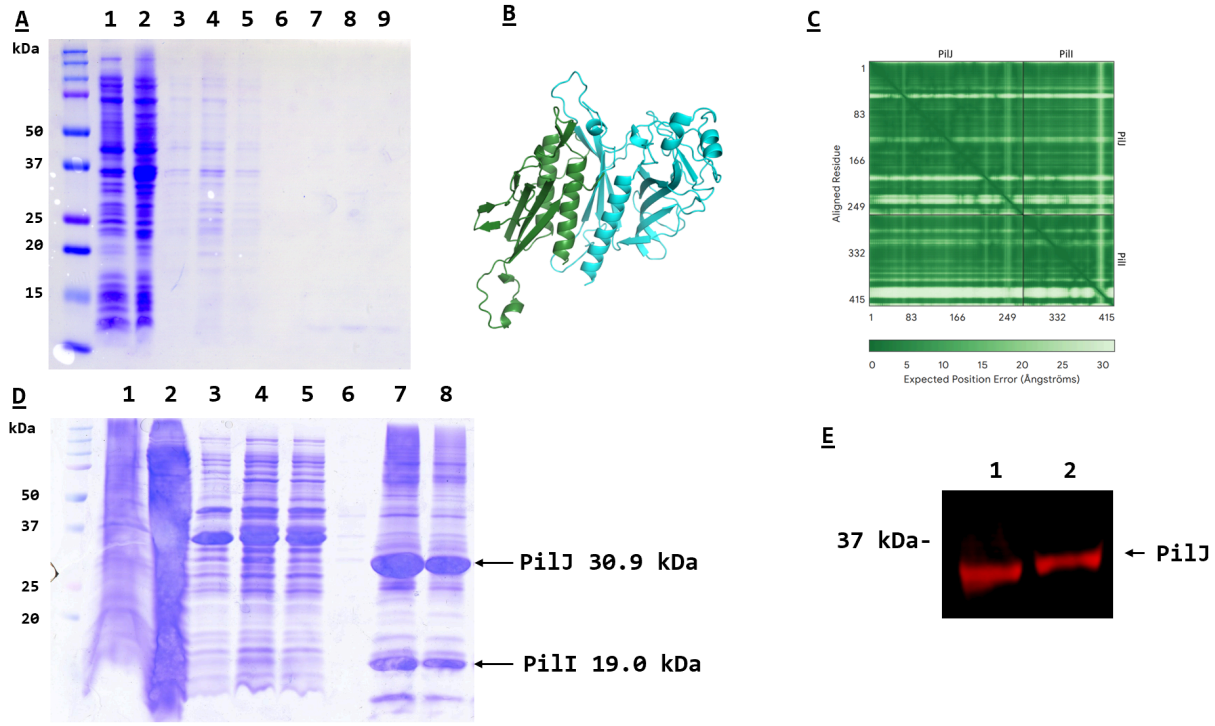

Figure 2-3 Expression and partial purification of a soluble PilI-PilJ complex.
A. Expression and failed purification of soluble engineered PilJ-His_6. Lane 1: pre-induction cell lysate. Lane 2: Post-induction cell lysate. Lane 3: sucrose shock supernatant. Lane 4: $MgSO_4$ supernatant. Lane 5: affinity resin flowthrough of the pooled shock supernatants. Lane 6: final affinity resin wash. Lanes 7-9: affinity resin eluate fractions.
B. Alphafold3 prediction of heterodimer formation between truncated PilI (Green) and PilJ (Cyan) soluble domains.
C. Alphafold3 confidence matrix for the predicted soluble PilI-PilJ heterodimer.
D. Purification of PilI $PilJ_{Short}$-His_6. Lane 1: pre-induction cell lysate. Lane 2: post-induction

cell lysate. Lane 3: sucrose shock supernatant. Lane 4: $MgSO_4$ shock supernatant. Lane 5: affinity resin flowthrough of the pooled shock supernatants. Lane 6: Final affinity resin wash. Lanes 7 and 8: Eluted $PilJ_{Short}$-His_6 complex.
E. Expression of engineered soluble minor pilin $PilJ_{Short}$-His_6, co-expressed with engineered soluble PilI, was analyzed by anti-His_6 immunoblot. Lane 1: whole cell lysate. Lane 2: periplasmic fraction.

2.6 Acknowledgments

J.N.A. was supported by the University of Washington STD & AIDS Research Training Program (NIH T32 AI07140). This work was supported by the National Institutes of Allergy and Infectious Disease (NIAID) R21 AI155991 and a kind gift to the UW Bacterial Research Fund from Professor J.M. Griffiss.

Table 2-S1 Plasmids used in this study.

Plasmid	**Description**	**Sequences of translated open reading frames** Non-native amino acid sequences are underlined.
AMP 2303	PilK-His_6	MRKQNTLTGIPTSDGQRGSALFIVLMVMIVVAFLVVPGAQASDNTEQRISANESDRKLALSLAEAALREG EFQVLDLEYTADSKVTFSENCEKGLCTAVNVRTNNNGNEEVFGNIVVQGTPTVEAVKRSCPAKSGKNSTG LCIDNQGVEYEKGTGNVSKMPRYIIEYLGEKNNQNIYRVTAKAWGKNANTVVVLQSYVGNNDEQGSGR SPGENLYFQGHHHHHH
AMP 2302	PilI-His_6	MKNNDCLRLKNPQSGMALIEVLVAMLVLTIGILALLPGAQASETQTIVSQITQNLMEGMLINPTIDSDSNK KNYNLYTGSYAPTSSDGDFKLNNLISKTDLAKAQLDRFGYELKQALPDAVAIRYAVCKDSSGDAPTLSGN TFSSNCDKKANGDTLIKVLWVNDSAGDSDIFRTNLEVSGSNIVYTYQARVGGREGSGRSPGENLYFQGHH HHHH
AMP 2305	PilJ-His_6	MKRKMLNVPKGGYDGMKGFTIVEFLVAGLLSVIVLIPGAQASETYFTSRKLNDAANERLAEQQDLRNAA TLIVRDARMAGSFGCFNMSEHIGNDVVFNVAQKNALFSLKRNSTNSTNKLIPITESPNINYQNFFQVSSALI FQYGIDDVDASADTTVVSSCAAISKPGKQIPTLENAKKELKIQNSDKEQNGNIARQRHVVNAYAVGKIAG EEGLFRFQLDDKGKWGNPQLLAKKVKRMRVRYIYVSGCPEDEDAGKEEQFKYTDKFDSSVTPAGVEVL LDSGSDAKIAASSDNIIYAYRINATIRGGNVCANRTLGSGRSPGENLYFQGHHHHHH
AMP 2352	$PilJ_{short}$-His_6	MKRKMLNVPKGGYDGMKGFTIVEFLVAGLLSVIVLIPGAQADENLAEQQDLRNAATLIVRDARMAGSFG CFNMSEHIGNDVVFNVAQKNALFSLKRNSTNSTNKLIPITESPNINYQNFFQVSSALIFQYGIDDVDASADT TVVSSCAAISKPGKQIPTLENAKKELKIQNSDKEQNGNIARQRHVVNAYAVGKIAGEEGLFRFQLDDKGK WGNPQLLAKKVKRMRVRYIYVSGCPEDEDAGKEEQFKYTDKFDSSVTPAGVEVLLDSGSDAKIAASSDN IIYAYRINATIRGGNVCANRTLGSGRSPGENLYFQGHHHHHH
AMP 2374	PilI + $PilJ_{short}$-His_6	MKNNDCLRLKNPQSGMALIEVLVAMLVLTIGILALLPGAQASETQTIVSQITQNLMEGMLINPTIDSDSNK KNYNLYTGSYAPTSSDGDFKLNNLISKTDLAKAQLDRFGYELKQALPDAVAIRYAVCKDSSGDAPTLSGN TFSSNCDKKANGDTLIKVLWVNDSAGDSDIFRTNLEVSGSNIVYTYQARVGGRE MKRKMLNVPKGGYDGMKGFTIVEFLVAGLLSVIVLIPGAQADENLAEQQDLRNAATLIVRDARMAGSFG CFNMSEHIGNDVVFNVAQKNALFSLKRNSTNSTNKLIPITESPNINYQNFFQVSSALIFQYGIDDVDASADT TVVSSCAAISKPGKQIPTLENAKKELKIQNSDKEQNGNIARQRHVVNAYAVGKIAGEEGLFRFQLDDKGK WGNPQLLAKKVKRMRVRYIYVSGCPEDEDAGKEEQFKYTDKFDSSVTPAGVEVLLDSGSDAKIAASSDN IIYAYRINATIRGGNVCANRTLGSGRSPGENLYFQGHHHHHH

Table 2-S2 Iterative process for SPI site redesign of PilK.

Changes made to the amino acid sequence in each iteration of design are highlighted in yellow. The predicted probabilities of SPI cleavage, estimated using SIGNALP5.0, are shown.

Construct	**SPI cleavage probability**	**N-terminal sequence**
Wild Type PilK	0.064	MRKQNTLTGIPTSDGQRGSALFIVLMVMIVVAFLVVTAAQSYNTEQRISAN…
Add A	0.1739	MRKQNTLTGIPTSDGQRGSALFIVLMVMIVVAFLVVTAAQASYNTEQRISAN…
Replace T->P	0.458	MRKQNTLTGIPTSDGQRGSALFIVLMVMIVVAFLVVPAAQASYNTEQRISAN…
Replace A->G	0.4654	MRKQNTLTGIPTSDGQRGSALFIVLMVMIVVAFLVVPGAQASYNTEQRISAN…
Replace Y->D	0.6444	MRKQNTLTGIPTSDGQRGSALFIVLMVMIVVAFLVVPGAQASDNTEQRISAN…

Chapter 3. β-strand complementation within tip initiation complexes licenses assembly of diverse type IV filaments

Chapter 3 is adapted with minimal modification from:

β-strand complementation within tip initiation complexes licenses assembly of diverse type IV filaments

Taylor J. Ellison, Zoey R. Litt, Justin N. Applegate, Emma Miller, Luther Davis, Alfredo Ruiz-Rivera, Angela Lisovsky, Rittika Saha, Naveen Jasti, Stephanie McLaughlin, Beth Traxler, Courtney K. Ellison, Alexey J. Merz

bioRxiv 2026.02.14.705861; doi: https://doi.org/10.64898/2026.02.14.705861

This chapter is the result of a collaborative effort. My contribution to this chapter includes the expression of minor pilins and Pilk-PilC co-purification outlined in section 3.4.2 PilK and PilC, and PilI and PilJ, form heterodimers, A. Lisovsky and I extensively optimized PilC expression, purification, and storage conditions, and I co-supervised the work of undergraduate researchers on minor pilin expression and purification.

3.1 Abstract

PilC/PilY1 proteins are tip-located adhesins of type IV pili (T4P) that are critical for T4P function in diverse behaviors including twitching motility, DNA uptake, and host cell adhesion. PilC and PilY1 adhesins are proposed to interact with initiation complexes composed of minor pilins (PilIJK family proteins) to aid in initiation of T4P polymerization, but it has been unclear how PilC/PilY1 proteins promote fiber assembly. We combined structural modeling, genetic, and biochemical experiments using *Neisseria gonorrhoeae* and *Acinetobacter baylyi* to delineate how PilC/PilY1 control T4P assembly: a short peptide at the C-terminus of PilC/PilY1 initiates T4P assembly via β-strand complementation with PilK-family minor pilins. This β-strand is necessary

and partially sufficient to trigger fiber assembly. In a working model, the PilK-PilC/PilY1 complex is recognized by a preformed PilI-PilJ heterodimer to form a quaternary "licensing complex" that then templates and initiates fiber assembly. In type II secretion systems (T2SS) lacking PilC/PilY1, PilK homologs directly incorporate the terminal β-strand provided by PilC/PilY1 in T4P. Moreover, phylogenetically distinct Tad T4P lack a canonical PilK homolog and instead contain a structurally similar minor pilin-like protein called TadG/CpaL that is important for fiber assembly. We show that CpaL of *Caulobacter crescentus* Tad T4P acts similarly to the T2SS PilK homolog to provide the C-terminal β-strand required for assembly. Our results explain how PilC/PilY1 can be retained on the fiber tip under enormous tensile loads generated during mechanical shear and T4P retraction and demonstrate how diverse T4P systems employ β-strand complementation to license fiber assembly.

3.2 Significance

Prokaryotic type 4 filaments are ancient, diverse, and broadly distributed nanomachines that assemble and retract extracellular protein filaments. They include type IV pili and type II secretion systems, mediating toxin secretion, motility, surface adhesion, biofilm formation, DNA uptake, and other functions. Here, we show that two widely conserved subunits of the tip, PilI and PilJ, form a module that recognizes the folding of a β-sheet in a third subunit, PilK. The final β-strand in this sheet can be supplied *in trans* by the last ~10 aminoacyl residues of large PilC/PilY1 adhesins, or *in cis* by PilK itself. In a working model, this recognition results in formation of a PilIJK trimer, which then licenses fiber polymerization through a templating mechanism.

3.3 Introduction

The type IV filaments (T4F) of Bacteria and Archaea are related, dynamic machines that reversibly assemble filamentous polymers to execute diverse functions including surface attachment and motility, DNA uptake, virulence, and protein secretion (Craig et al. 2019; Korotkov and Sandkvist 2019). The T4F superfamily comprises diverse microbial appendages including type IV pili (T4P), mannose-sensitive hemagglutinin (MSHA) pili, type II secretion systems (T2SS), and the archaellum used for archaeal swimming motility (Denise et al. 2019; C. K. Ellison et al. 2022). Bacterial T4P can further be subdivided: T4aP, T4bP, and Tad T4cP are distinguished by differences in pilin subunit leader sequence length and homologies among assembly components (Denise et al. 2019). The competence (Com) pili of Gram-positive species form extended filaments and are now classified as T4dP (T. Lam et al. 2021; Laurenceau et al. 2013; Jeremy Mom et al. 2024; Jérémy Mom et al. 2025; Zuke et al. 2023). Most T4F share the ability to dynamically extend and retract. T4F dynamics are driven by cyclical polymerization and disassembly of pilin subunits from a cytoplasmic membrane pool (Bradley 1974; Charles-Orszag et al. 2024; Francetic et al. 2007; Koch et al. 2022; A. J. Merz et al. 2000; Alexey J. Merz and Forest 2002; Skerker and Berg 2001). While extension and retraction dynamics are crucial for most T4F functions, archaella are instead rotated to power swimming, similar to Bacterial flagella.

Pilin subunits are added and removed from the fiber base. Polymer initiation relies on minor pilin initiation complexes at the filament apical tip. However, the assembly sequences and quaternary structures of these complexes are opaque (Guo et al. 2024; Nguyen et al. 2015; Treuner-Lange et al. 2020; Hanne C. Winther-Larsen et al. 2005). T4P tip complexes commonly comprise three or more distinct minor pilin subunits, each structurally similar to the major pilin

that comprises the bulk of the fiber. Pilins fold into a "lollipop" structure with a conserved N-terminal hydrophobic domain and a C-terminal globular domain that is structurally more variable. The N-terminal α-helical domain anchors unassembled pilins in the cytoplasmic membrane, and forms the structural core of the polymerized fiber. The globular C-terminal domain is more exposed to the environment and contributes to the functional diversity of the T4F superfamily. Minor pilin initiation complexes are hypothesized to function analogously to eukaryotic Arp2/3 and γ-tubulin ring complexes that initiate actin filament and microtubule polymerization (Mullins et al. 1998; Kollman et al. 2011; Rotty et al. 2013). In each case, an oligomer of subunits homologous to the major protomer is hypothesized to nucleate polymerization through a templating mechanism. Templating increases the rate of polymer initiation by overcoming rate-limiting thermodynamic barriers that impede spontaneous nucleation. Arp2/3 and γ-tubulin complexes further act as signal integrators that license filament polymerization in response to specific cues. T4P tip complexes may have analogous functions.

In addition to minor pilins, T4aP tips often incorporate large adhesins of the PilC/PilY1 family (Alm et al. 1996; Jonsson et al. 1991; Nassif et al. 1994; Nguyen et al. 2015; Wolfgang et al. 1998). In mutants lacking individual minor pilins or PilC/PilY1, many species including *Neisseria gonorrhoeae*, *Pseudomonas aeruginosa*, *Acinetobacter baylyi*, and *Myxococcus xanthus* are nearly devoid of pili at steady state. Removal of PilT, the retraction motor ATPase that powers depolymerization of the pilus fiber, traps pili in the assembled state and suppresses these steady-state defects in piliation (Bradley 1974; A. J. Merz et al. 2000; Whitchurch et al. 1991; Hanne C. Winther-Larsen et al. 2005; Wolfgang et al. 1998). An obvious inference is that minor pilins and PilC/PilY1 are required for efficient polymer initiation, but dispensable for processive filament polymerization or depolymerization.

PilC/PilY1 translocate across the cytoplasmic membrane through the SecYE/signal peptidase I pathway. They have structurally diverse N-terminal adhesin domains but share a conserved C-terminal β-propellor domain (Orans et al. 2010). They usually contain several disulfide bonds. N-terminal adhesin domains can be over 3,000 residues long, and are hypothesized to encompass diverse adhesin activities. Some evidence indicates that the C-terminal β-propellor is sufficient to support pilus assembly (Sacharok et al. 2022), and recent structural results prompted speculation that PilC/PilY1 has a role in gating of the outer membrane secretin bushing, through which the assembled fiber passes (Guo et al. 2024). However, the structure of the tip complex and the molecular mechanism(s) through which PilC/PilY1 controls fiber initiation have remained unclear. We now present molecular modeling, genetic, and biochemical evidence that a ~6-10 amino acid assembly signal at the extreme C-terminus of PilC/PilY1 (Cβ) licenses formation of the core minor pilin trimer PilIJK through a β-strand complementation with PilK-family minor pilins. The PilK-PilC/PilY1 heterodimer is then recognized by a pre-formed PilI-PilJ heterodimer. Licensing by Cβ is necessary, and PilK-Cβ fusions are at least partially sufficient to initiate fiber assembly and elongation. Structural modeling suggests that diverse T4F use this β-strand complementation for tip complex formation. In line with this prediction, we show the minor pilin-like protein CpaL found in Tad T4cP behaves similarly to GspK in T2SSs, providing the β-strand required for complex assembly. To our knowledge, this is the first example of a specific polymerization signal for any T4F system.

3.4 Results

Initiation tip complex protein nomenclature varies across T4F systems. For example, the *N. gonorrhoeae* minor pilins PilH, PilI, PilJ, and PilK correspond to FimT/U, PilV, PilW, and PilX in *P. aeruginosa*. We use existing annotations (except for the PilW/GspJ protein ComB in *A. baylyi*, here referred to as PilW). The names of homologous subunits in different T4F systems are shown in **Table 3-1 and Fig. 3-S1.**

Table 3-1. Core initiation tip complex homologs across different species and T4F systems

T2SS	T4aP *Ngo*	T4aP *Ab*	T4aP *Pa*	Com *Bs*	T4aP *Vc*	MSHA *Vc*	T4cP *Cc*
GspI (XcpV)	PilI	PilV	PilV	ComGE	PilV	MshD	CpaK
GspJ (XcpW)	PilJ	PilW (ComB)	PilW	ComGF	PilW	MshO	CpaJ
GspK (XcpX)	PilK	PilX	PilX	**ComGG**	**PilX**	MshP	**CpaL**
–	**PilC**	**PilY1**	**PilY1**	–		**MshQ**	

Bold text indicates the protein proposed to supply the terminal β-strand required for complex assembly. *Ngo, Neisseria gonorrhoeae; Ab, Acinetobacter baylyi; Pa, Pseudomonas aeruginosa; Vc, Vibrio cholerae; Bs, Bacillus subtilis; Cc, Caulobacter crescentus. The assignments are based on reported homologs, protein sequence alignments, structural features, and AlphaFold modeling of tip complexes.*

3.4.1 A PilC/PilY1 C-terminal peptide is predicted to strand-complement the β-sheet in GspK homologs.

AlphaFold3 modeling of PilC/PilY1 complexes found in T4aP with core minor pilins yielded consistent predictions for the arrangement of PilI, PilJ, PilK, and PilC/PilY1 across many species including: *Neisseria gonorrhoeae*; *Acinetobacter baylyi*; *Pseudomonas aeruginosa*; and *Myxococcus xanthus*. A model of the *N. gonorrhoeae* tip complex is shown in **Fig. 3-1.** Additional T4aP models are shown in **Fig. 3-S2**. **Figs. 3-S3** through **3-S6** show confidence metrics for the structural predictions. In every case, PilI, PilJ, and PilK are arranged in clockwise order when viewed from above the complex's apical tip (**Fig. 3-1A**). This predicted structural conservation parallels observations that the polycistronic organization of *pilI*, *pilJ*, and *pilK* genes is almost invariably syntenic across T4aP and T2SS (Hanne C. Winther-Larsen et al. 2005) (**Fig. 3-S1**).

The conserved PilC/PilY1 β-propellor is predicted to sit atop the minor pilin PilIJK heterotrimer, with variable orientations in different models. However, in every case the extreme C-terminus of PilC/PilY1 (~10 aminoacyl residues) penetrates down the centerline of the PilI-J-K heterotrimer at the PilJ-PilK assembly interface (**Fig. 3-1A, Fig. 3-S2**). In each case the PilC/PilY1 C-terminal peptide is predicted to strand-complement the small β-sheet in PilK, and lies in a complementary groove in PilJ (**Fig. 3-1A**). Solved crystal structures of the T2SS tip complexes of *Escherichia coli* (GspIJK) and *Pseudomonas aeruginosa* (XcpVWX), topologically mirror the predicted T4P tip complex (Korotkov and Hol 2008; Zhang et al. 2018). Remarkably, in the T2SS structures the conserved C-terminal β-strand, rather than being provided by a tip adhesin, is itself the C-terminal β-strand of the PilK homologs GspK and XcpX (**Fig. 3-1B**).

This structural arrangement suggests a working model: stepwise association of the C-terminal PilC/PilY β-strand with the beta sheet in the globular domain of PilK is followed by recognition of this heterodimer by PilJ and PilI. Deep burial of the PilC/PilY1 C-terminal β-strand appears to rule out models in which PilC/PilY1 associates with a pre-formed PilI-J-K heterotrimer. The large buried area of the PilC β-strand in the predicted *N. gonorrhoeae* PilI-J-K complex (~1700 Å^2 for the example in **Fig. 3-1A**) would provide mechanical stability required to withstand enormous tensile forces (≥100 pN) developed during pilus retraction or when cells encounter hydrodynamic shear forces (Maier et al. 2002; A. J. Merz et al. 2000).

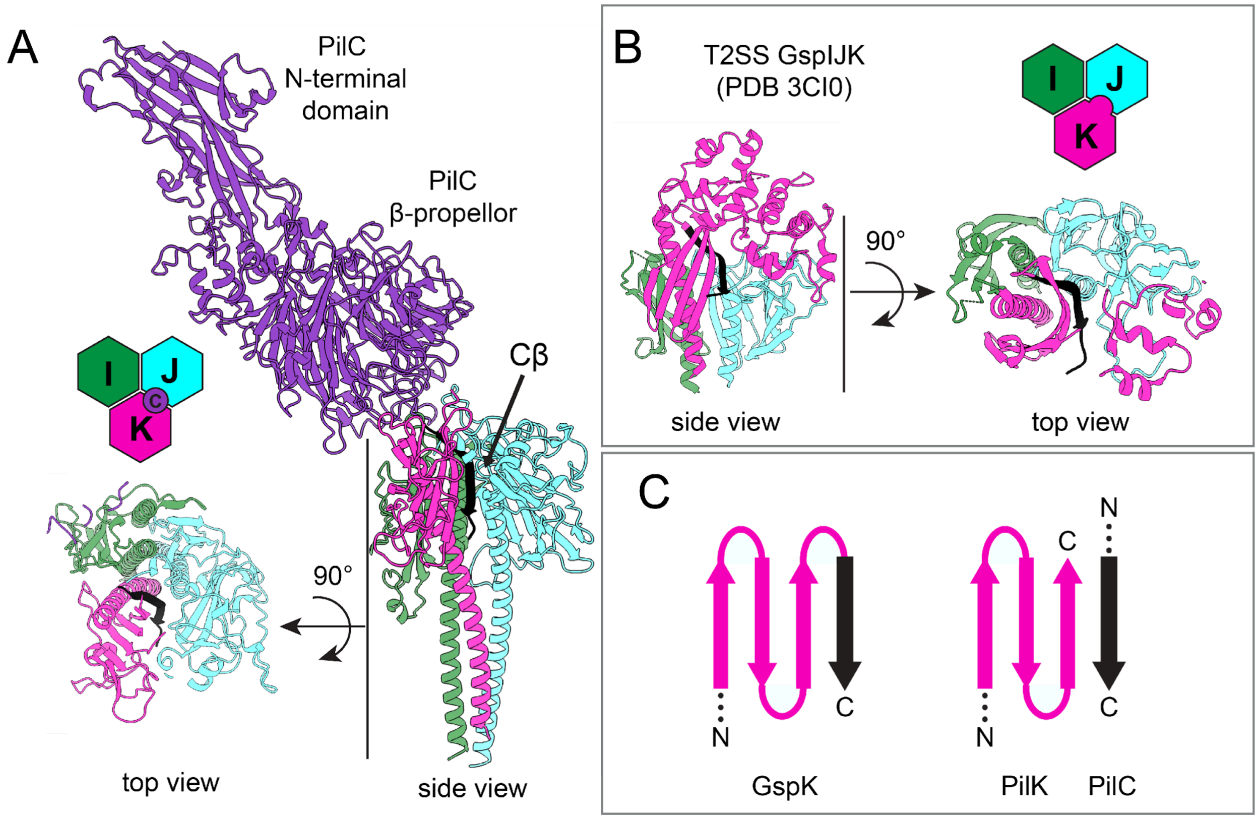

Figure 3-1. A β-strand completes the β-sheet in PilK homologs.
(A) AlphaFold model of *N. gonorrhoeae* PilIJK minor pilins in complex with the tip adhesin PilC. The PilC C-terminal β-strand (black) completes the PilK β-sheet *in trans*. (B) Crystal structure of the T2SS minor pilin complex (PDB 3CI0) from enterotoxigenic *E. coli*. In T2SS initiation complexes, the complementing β-strand is provided by GspK itself. (C) Schematic of the β-strand complementation model. In all figure panels, the conserved C-terminal β-strand is colored black.

3.4.2 PilK and PilC, and PilI and PilJ, form heterodimers

PilK and its homologs are predicted to be the most apical minor pilins in the tip complex, as they invariably lack a conserved +5 Glu residue critical for interactions with the N-terminal regions of previously incorporated (more apical) pilin subunits. Coupled with the prediction that the PilC/PilY1 β-strand mimics the C-terminal β strand of GspK in T2SS (which lack PilC/PilY1), we hypothesize that PilC/PilY1 and PilK form a heterodimer that assembles prior to PilI-PilJ incorporation. To test whether PilK and PilC/PilY1 can form a heterodimeric structure, we co-expressed periplasmic, soluble *N. gonorrhoeae* PilK-His_6 (Applegate et al. 2026) and the conserved C-terminal half of PilC, bearing a cleavable N-terminal signal peptide and FLAG tag (ΔN-FLAG-PilC) in *E. coli* cells. SDS-PAGE followed by silver stain of periplasmic fractions revealed co-elution of PilK and PilC, which were verified by immunoblot (**Fig. 3-2A**). Thus, as predicted by our modeling, PilK directly binds to the C-terminal half of PilC. The binding of ΔN-FLAG-PilC was sub-stoichiometric, likely due to differences in expression of PilK-His_6 from a high copy plasmid and ΔN-FLAG-PilC from a low-copy plasmid. It is also possible that the PilK-PilC complex is of only moderate affinity and partially dissociates during purification.

The T2SS GspI and GspJ minor pilins are adjacent in crystal structures (Korotkov and Hol 2008; Yanez et al. 2008; Zhang et al. 2018). In our experiments, *N. gonorrhoeae* T4aP minor pilins PilI and PilJ formed a heterodimer stable through affinity co-purification (Applegate et al. 2026) and size exclusion chromatography (**Fig. 3-2B**). Notably, addition of PilK to the heterodimeric sample did not result in a shift in the PilI-PilJ elution curve (**Fig. 3-2C**). In *N. gonorrhoeae*, deletion of either PilI or PilJ results in loss of both proteins, without affecting the stability of other minor pilins or PilC (Hanne C. Winther-Larsen et al. 2005). Moreover, PilJ alone could not be purified, while co-expression with PilI allowed PilJ purification (Applegate et

al. 2026). Together these results indicate that PilI and PilJ interact to form a stable, obligate heterodimer. We therefore propose that a pre-assembled PilI-PilJ heterodimer in turn recognizes formation of the PilC/PilY1 complex. PilC/PilY1 proteins are large. *A. baylyi* PilY1 is ~1500 residues long and has ten predicted disulfide bonds. Metagenomic sequences identify PilC/PilY1 family members of up to 3500 residues. We surmise that cells must ensure that PilC/PilY1 is synthesized, translocated into the periplasm, and folded before being mounted at the tip of an elongating T4P. Licensing of initiation complex assembly by the extreme C-terminus of PilC/PilY1 would satisfy this requirement.

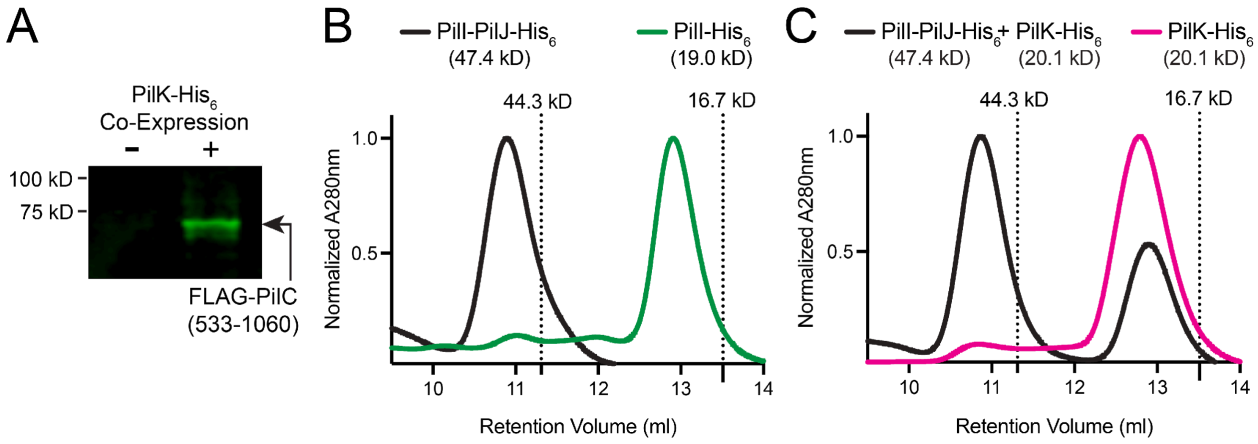

Figure 3-2. PilK and PilC, and PilI and PilJ, form heterodimers.
(A) Co-Purification of periplasmically expressed ΔN-FLAG-PilC(533-1060) when PilK-His_6 is captured by immobilized metal chromatography. Eluates were immunoblotted with anti-FLAG antibodies to detect FLAG-tagged PilC. ΔN-FLAG-PilC(533-1060) was expressed in the absence (lane 1) or presence (lane 2) of PilK-His_6. (B) Size exclusion chromatography (Superdex 75 Increase) of soluble PilI-PilJ-His_6 heterodimer (black) or PilI-His_6 alone (green). (C) Size exclusion chromatography (Superdex 75 Increase) of purified soluble PilI-PilJ-His_6 and PilK-His_6 proteins mixed together (black) and PilK-His_6 alone (pink). In figures (B) and (C), A280nm values are normalized to the maximum peak of each trace. Expected masses of the protein complexes are indicated in parentheses. Dashed lines indicate elution peaks for standards: ovalbumin (44.3 kDa) myoglobin (16.7 kDa). Each trace is representative of n=3 independent replicates.

3.4.3 The C-terminal peptide is essential and partially sufficient for PilC function

N. gonorrhoeae FA1090 encodes two redundant PilC/PilY1-encoding genes which appear to be functionally equivalent. In this strain *pilC1* is phase-varied on, while *pilC2* is phase-varied off. To simplify our experiments, we employed a Δ*pilC2* mutant background with *pilC1* phase-locked on (see strain table for details). Mutant cells lacking the 12-residue C-terminal peptide of PilC1 (*pilC1*Δ*Cβ*) phenocopied the Δ*pilC1* null mutant. Consistent with our hypothesis that the PilC/PilY1 β-strand is required for minor pilin complex licensing, T4P-labeling using cysteine knock-in maleimide-staining (C. K. Ellison et al. 2017; C. K. Ellison, Dalia, et al. 2019) revealed loss of fiber assembly in Δ*pilC1* and *pilC1*Δ*Cβ* mutants (**Fig. 3-3A, B**). Similarly, colony morphology resembled that of mutants lacking T4P (**Fig. 3-3C**). Natural transformation, which depends on T4P-mediated DNA uptake, was also abolished in the *pilC1*Δ *Cβ* mutant (**Fig. 3-3D**). The *pilC1*Δ*Cβ* allele exhibits partially dominant loss of function, so restoration of function *pilC1*Δ*Cβ* mutant cells through complementation *in trans* was not possible. Thus, we turned to amber suppression. Insertion of an amber stop codon *pilC1-Lys1051Amb* to truncate *pilC1* phenocopied the loss of piliation and DNA transformation caused by *pilC1*Δ*β* Expression of $tRNA^{Lys}_{Amb}$ rescued the DNA transformation defect *Lys1051Amb* by about 20-fold (**Fig. 3-3E**). To our knowledge this is the first use of tRNA suppression in *Neisseriaceae*. We anticipate that future work will result in systems capable of more efficient suppression, as well as incorporation of noncanonical amino acids.

In crystal structures of the T2SS PilK ortholog GspK, an additional C-terminal β-strand is present, at the location where the last ten residues of PilC/PilY1 are predicted to engage in β-strand complementation with PilK (**Fig. 3-1**). We therefore speculated that fusion of the last ~10-20 residues of PilC to the C-terminus of the minor pilin PilK might compensate for loss of

PilC/PilY1. AlphaFold modeling confidently predicted a fusion of the terminal residues from PilC to the C-terminus of PilK could form a stable complex, with the fused C-terminal β-strand positioned between PilK and PilJ in the same location as the wild-type PilC C-terminal β-strand (**Fig. 3-3E**). We constructed a Δ*pilC1* strain where the terminal 12 residues from PilC1 were appended to the extreme C-terminus of PilK (annotated here as *pilK-Cβ*) (**Fig. 3-3E**). While the Δ*pilC1* mutant produced no visible T4P, and T4P were only observed in a single replicate of the *pilC1*Δ*Cβ* strain experiments, T4P were apparent in 3 of 4 biological replicates for the *pilK-Cβ* strain suggesting an increase in piliation versus the *pilC1* mutants (**Fig. 3-3A, B**). Although this difference was not statistically significant, long pili are relatively rare and the limit of detection by fluorescence microscopy is <250 nm, limiting detection of shorter fibers (Kraus-Römer et al. 2022). To test whether the *pilK-Cβ* strain might produce an increase in functional but short T4P we performed natural transformation assays. The *pilK-Cβ* allele increased transformation frequency by more than four orders of magnitude versus the Δ*pilC1* null allele, reaching almost wild-type efficiency (**Fig. 3-3C**). Thus, the last 12 residues of PilC are partially sufficient for pilus initiation and function when full-length PilC is completely absent.

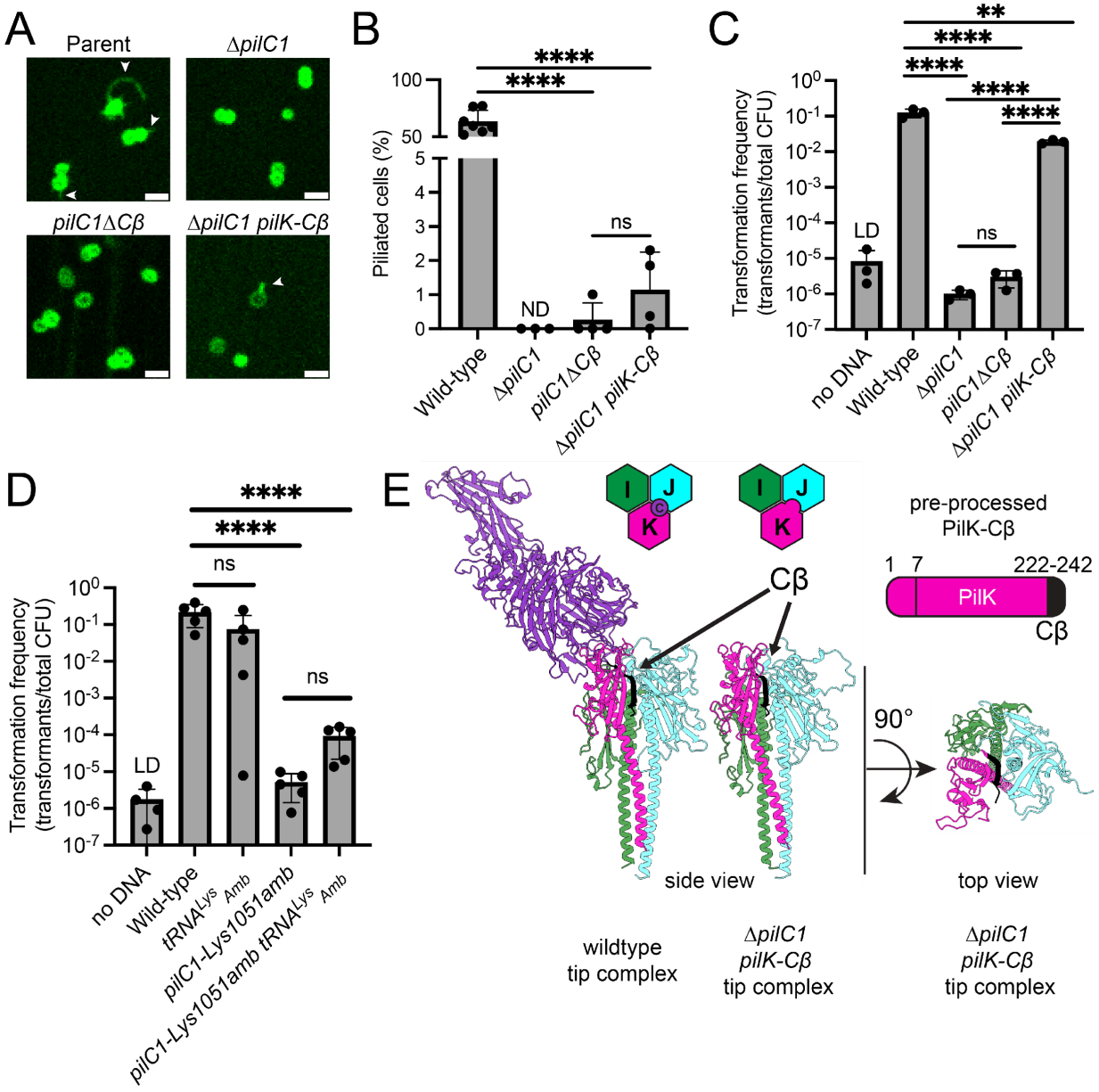

Figure 3-3. The extreme C-terminus of PilC is essential and partially sufficient for its function in *N. gonorrhoeae*.

(A) Representative microscopy images of indicated strains. White arrows indicate examples of visible T4P filaments. Scale bars, 2µm. (B) Quantification of piliated cells in populations of strains shown in (A). Bar graph shows the mean +/- SD. Each dot represents an independent, biological replicate. ND, not detected. (C) Natural transformation assay data from indicated strains. (D) Natural transformation assay data from amber supression. Bar graph shows the mean +/- SD. Each dot represents an independent, biological replicate. (E) AlphaFold models of T4P tip complexes from indicated strains. Top right shows a schematic of the pre-processed form of the PilK-Cβ fusion. Statistical analysis for natural transformation assays was performed on log-transformed transformation frequency data. ANOVA tests were corrected for multiple comparisons using Sidak's method. ****P<0.0001; **P<0.005; ns, not significant; LD, limit of detection.

3.4.4 The PilC/PilY1 β-strand's function is conserved

To determine whether the C-terminal β-strand of PilC1/PilY1 functions similarly in other T4aP systems, we used *Acinetobacter baylyi* as a model organism to represent the well-studied T4P found in the *Pseudomonadales* order, which includes *P. aeruginosa* and closely related *Acinetobacter* pathogens. Similar to *N. gonorrhoeae* T4aP, AlphaFold modeling predicted that the extreme C-terminal residues of PilY1 form a β-strand that completes the β-sheet of PilX, the *A. baylyi* PilK homolog (**Fig. 3-4A, 3-S2, 3-S4**). As in *N. gonorrhoeae*, C-terminal β-strand deletion from PilY1 in *A. baylyi* phenocopied the Δ*pilY1* deletion and caused loss of pilus assembly (**Fig. 3-4B, C**). In *A. baylyi*, we observed a significant increase in piliation in a Δ*pilY1 pilX-Cβ* strain (**Fig. 3-4C**). Natural transformation experiments also indicated restoration of pilus function, with the Δ*pilY1 pilX-Cβ* strain showing a ~10^4-fold increase over the Δ*pilY1* strain, exactly mirroring our experiments with *N. gonorrhoeae*. (**Fig. 3-4D**). Together, our data demonstrate that the final ~10 residues of PilC/PilY1 are necessary and partially sufficient for tip complex function in T4aP.

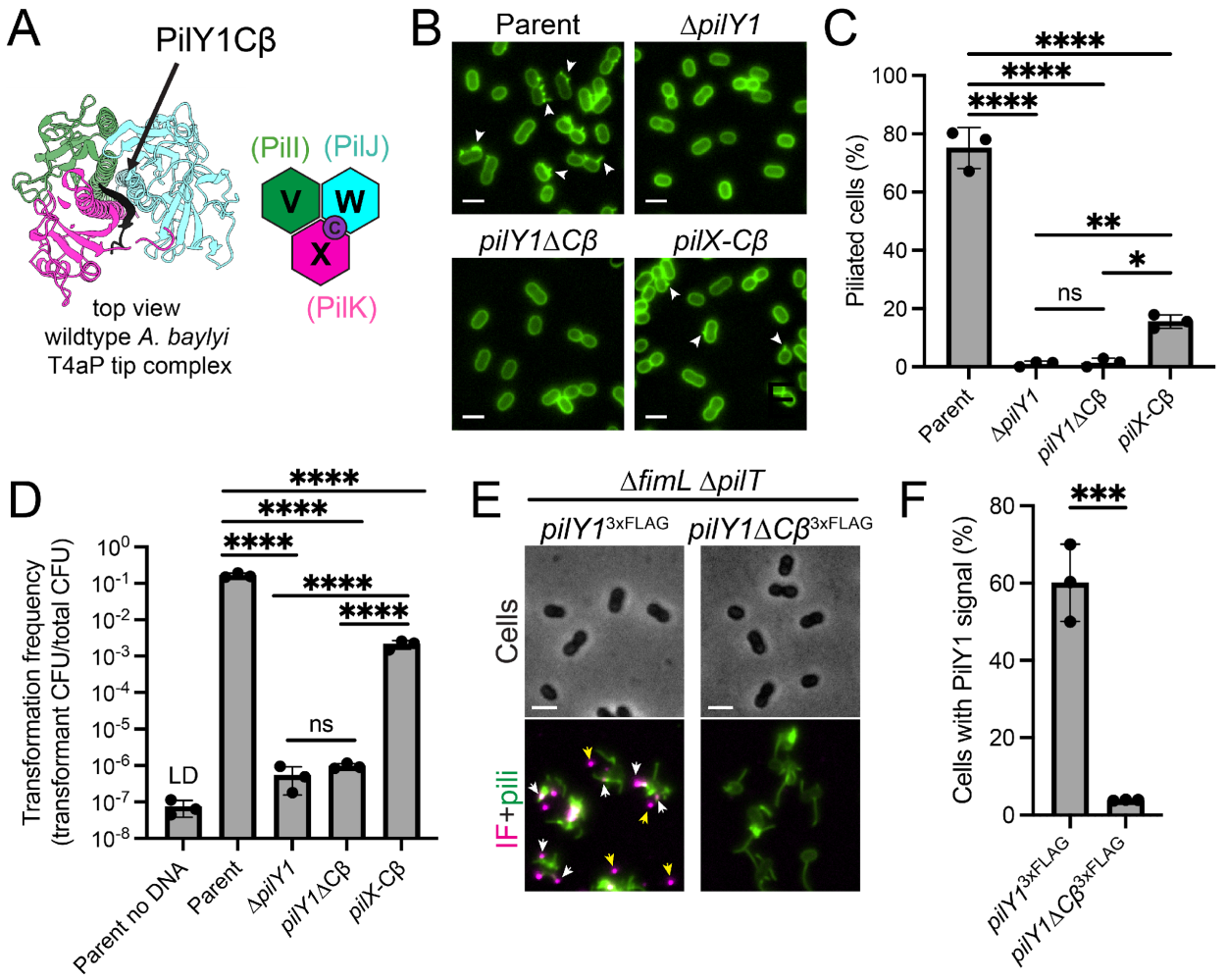

Figure 3-4. The extreme C-terminus of PilY1 is essential and partially sufficient for its function in other T4aP systems.

(A) Top view of the AlphaFold model of the wildtype T4P tip complex from *A. baylyi*. (B) Representative microscopy images of indicated strains with background fluorescence subtracted. White arrows indicate examples of visible T4P filaments. (C) Quantification of piliated cells in populations of strains shown in (B). Bar graph shows the mean +/- SD. Each dot represents an independent, biological replicate. (D) Natural transformation assay data from indicated strains. Bar graph shows the mean +/- SD. Each dot represents an independent, biological replicate. (E) Representative microscopy images of indicated strains with background fluorescence subtracted. IF, immunofluorescence signal. White arrows represent examples of PilY1 associated with individual cells. Yellow arrows indicate sheared PilY1 that is not associated with cells. (F) Percentage of cells with associated PilY1 immunofluorescence signal of strains shown in (E). Bar graph shows the mean +/- SD. Each dot represents an independent, biological replicate. Statistical analysis for natural transformation assays was performed on log-transformed transformation frequency data. ANOVA tests were corrected for multiple comparisons using Sidak's method. ****P<0.0001; ***P<0.001, **P<0.01; *P<0.05; ns, not significant; LD, limit of detection. Scale bars, 2 µm.

3.4.5 The terminal β-strand stabilizes PilC/PilY1 at the filament tip

Because the C-terminal β-strand is predicted to anchor PilC/PilY1 to minor pilins in the tip complex, we reasoned that deletion of this peptide should prevent PilY1 association with the pilus tip. Using recently published immunofluorescence microscopy methods for labeling tip-associated minor pilins (T. J. Ellison and Ellison 2025; Sztanko et al. 2026), we tagged PilY1 and PilY1ΔCβ at the native locus with a 3xFLAG epitope and assessed whether cells exhibited associated PilY1 immunofluorescence signal (**Fig. 3-4E, F**). Although the 3xFLAG tag caused a ~1-$\log_{10}$ loss of function in natural transformation experiments, PilY1ΔCβ was present at similar levels as PilY1, showing that the C-terminal β-strand is not needed for PilY1 expression or stability *per se* (**Fig. 3-S7A, B**). Because *pilY1ΔCβ* mutant cells do not produce detectable T4P in cells where the PilT retraction ATPase is intact, we employed Δ*pilT* mutants to increase the amount of visible T4P for immunofluorescence studies. Additionally, *A. baylyi* produces its T4P close together in a line along the long axis of the cell making it difficult to resolve individual T4P, especially in hyperpiliated Δ*pilT* strains. Long-axis localization depends on the chemosensory Pil-Chp pathway (C. K. Ellison et al. 2022; T. J. Ellison et al. 2025), so we used a published Pil-Chp mutation (Δ*fimL*) to enhance detection of individual, extended T4P (**Fig. 3-4E, F**). Wild-type PilY1 associated with ~60% of cells versus ~4% of cells expressing PilY1ΔCβ, indicating that the C-terminal β-strand is important for PilY1 association with the T4P fiber (**Fig. 3-4E, F**). While we expect that all T4P tip complexes in the wild type incorporate PilY1, not all cells or T4P exhibited detectable PilY1 signal, as in minor pilin immunofluorescence studies (T. J. Ellison and Ellison 2025). This is likely due to shearing of T4P during the many wash steps in immunofluorescence sample preparation. Indeed, we

frequently observed of PilY1 signal not associated with cells, including sheared filaments with tip-associated PilY1 (**Fig. 3-4E, 3-S7C**).

3.4.6 Diverse T4Fs employ C-terminal β-strand complementation to stabilize tip complexes

T4P are broadly distributed structures that belong to the diverse T4F family composed of structurally related nanomachines. Detailed phylogenetic analysis of T4P and their homologs by Denise et al. 2019 shows T4F are so widely distributed that they may have been present in the last universal common ancestor (Charles-Orszag et al. 2024; Denise et al. 2019) (**Fig. 3-S8**). Evolution of the T4F family has led to diversification of these structures into multiple distinct subclades, some with dedicated functions as exemplified by Com T4dP found in competent Gram-positive bacteria that are used specifically for DNA uptake (**Fig. 3-S8**). Crystal structures and models of minor pilin trimers from T2SS and structural predictions of the tip complexes from other T4F provide support that β-strand complementation may promote tip complex licensing and stability in diverse systems (**Fig. 3-1B, Fig. 3-S9**). In systems where minor pilin homologs are present and readily identified (see Discussion for details), a C-terminal β-strand is present at the same location and orientation as the predicted PilC/PilY1 C-terminal β-strand in T4aP (see Fig. 3-S10 and 3-C11 for AlphaFold confidence metrics). The MSHA-encoding locus found in *V. cholerae* is not predicted to contain a PilY1 homolog, but the gene encoding the large (~1200 residue) protein MshQ is located immediately downstream of the *pilIJK* homologs *mshDOP*. *mshDOPQ* exhibit conserved gene synteny with T4aP systems encoding *pilVWXY1* in the *Pseudomonadales* order, indicating potential functional homology between these systems (**Fig. 3-S1**). AlphaFold modeling predicts that the extreme C-terminus of MshQ, like PilC/PilY1, engages in β-strand complementation with the PilK homolog MshP (**Fig. 3-S9**). This prediction is in accord with β-strand complementation regulating tip complex assembly in divergent T4P,

and suggests that AlphaFold modeling of tip complexes may enable identification of as-of-yet unidentified tip complex subunits.

Bacillus subtilis Com T4dP, and *V. cholerae* T4aP, both involved in DNA uptake, do not include a PilC/PilY1 ortholog. In each case the PilK ortholog has an additional β-strand, similar to T2SS GspK pilins. One of the most divergent subgroups of T4F include the Tad T4cP, which until recently were thought to contain only two minor pilin tip complex subunits (Charrouf et al. 2025). The minor pilin-like protein CpaL (~600 residues) was recently identified as a component of the *C. crescentus* Tad T4cP tip complex, playing an important role in bacterial surface sensing (Charrouf et al. 2025). Because Tad T4cP represent the most divergent evolutionary clade of Bacterial T4P, we reasoned that the presence of C-terminal β-strand complementation in this clade might suggest β-strand complementation as a mechanism present in the ancestral T4F system (**Fig. 3-S8**) (Denise et al. 2019). As in other T4F systems, AlphaFold modeling of CpaL with previously identified minor pilin subunits CpaJ and CpaK predicts that the extreme C-terminus of CpaL exhibits β-strand complementation with the β-sheet in its N-terminally located minor pilin-like domain (**Fig. 3-S9, 3-5A**). Additional AlphaFold modeling suggests that the middle ~470 residues of CpaL may be dispensable for tip complex stability, and predicts that a fusion of the extreme C-terminal six amino acids to the minor pilin-like domain might function like T2SS GspK or like our chimeric PilK/X-Cβ mutants. Using a hyperpiliated mutant of *C. crescentus* (C. K. Ellison, Kan, et al. 2019), we constructed Δ*cpaL* and *cpaL*Δ*Cβ* strains, as well as a strain lacking the middle region of CpaL at the native locus (Δmiddle) (**Fig. 3-5**). Similar to T4aP systems lacking the C-terminal β-strand, T4P were not detected in the Δ*cpaL* strain and were almost undetectable in the *cpaL*Δ*Cβ* mutant. In contrast, the Δmiddle strain produced

significantly more T4P, with piliation restored in almost 15% of the population (~38% of wild-type levels).

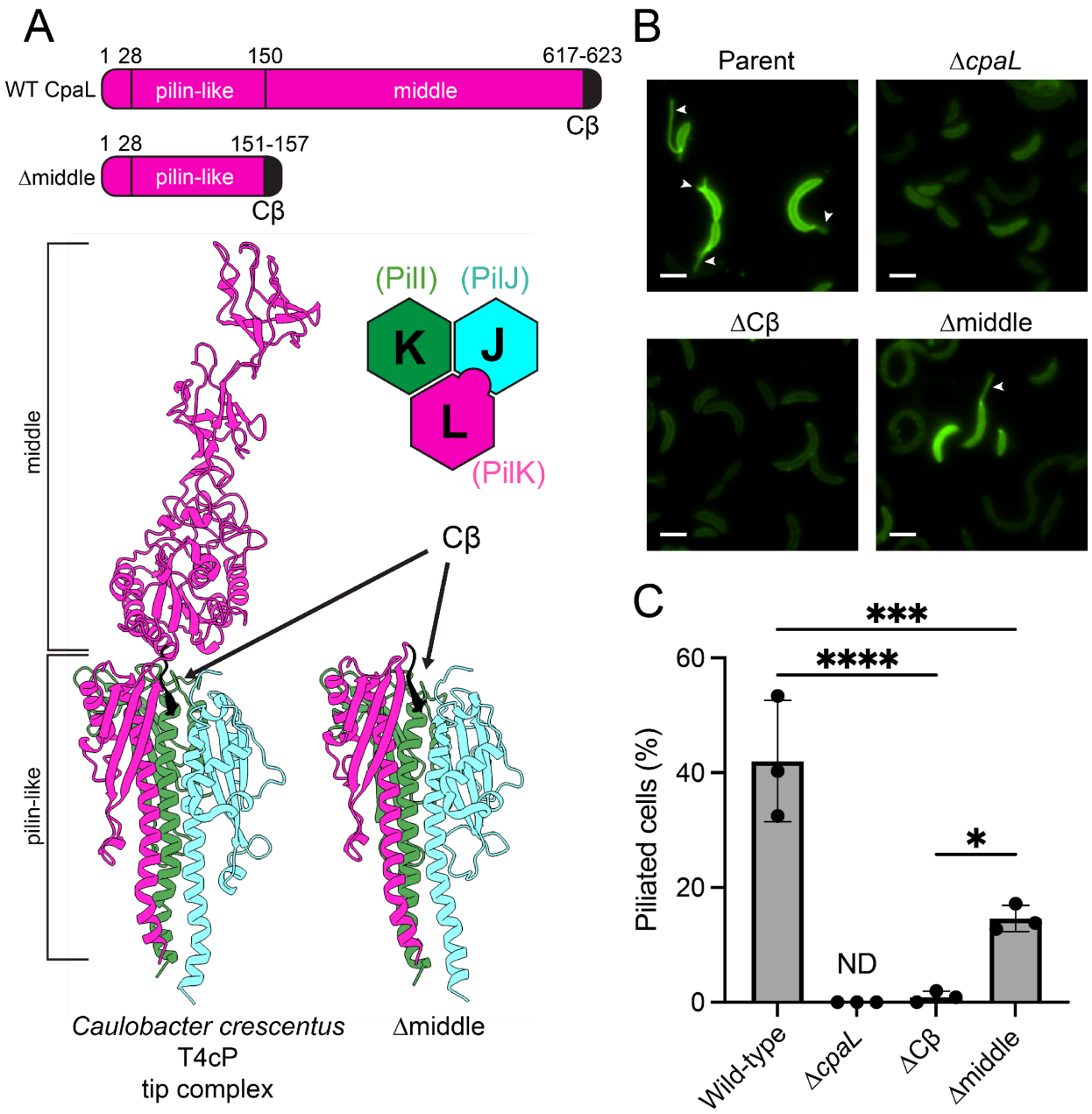

Figure 3-5. Diverse T4Fs employ C-terminal β-strand complementation to stabilize the tip complex.
(A) A schematic of wildtype CpaL (WT) compared to the Δmiddle strain lacking the internal ~470 residues predicted to sit atop the T4cP tip (top). AlphaFold models of the wildtype or Δmiddle tip complexes from *C. crescentus* CB13. In both models, the conserved C-terminal β-strand is colored black. (B) Representative microscopy images of indicated strains with background fluorescence subtracted. White arrows indicate examples of visible T4P filaments.

Scale bars, 2 μm. (C) Quantification of piliated cells in populations of strains shown in (B). Bar graph shows the mean +/- SD. Each dot represents an independent, biological replicate. ANOVA tests were corrected for multiple comparisons using Sidak's method. ****P<0.0001; ***P<0.001, *P<0.05; ND, not detected.

3.5 Discussion

Our results indicate that C-terminal β-strand complementation within diverse T4F tip complexes is important for initiating fiber polymerization, and might have been a feature of ancestral T4F systems. The T4F superfamily is among the most versatile and broadly distributed groups of nanomachines found in prokaryotes, and was likely present in the last universal common ancestor of life. Yet it is still unclear how these dynamic structures are regulated and what signals trigger initiation of fiber polymerization. In this work we uncovered a crucial aspect of fiber assembly by identifying β-strand complementation as a key mechanism of tip complex licensing and stability. We show β-strand complementation can be provided by either a tip-associated functional protein like those in the PilC/PilY1 family or by the most apical minor pilin (or minor pilin-like protein) in the complex, as is the case for T2SS and Tad T4cP. The conservation of β-strand complementation as a mechanism for promoting tip complex assembly between the distantly related Tad T4cP and other T4F suggests that ancestral T4F from which all modern T4Fs descended may have used a similar mechanism to promote fiber assembly (**Fig. 3-S8**).

Incomplete rescue of fiber initiation by PilK/X-Cβ chimeras suggests that PilC/PilY1 proteins have additional functions in T4P biogenesis and dynamics, and we suggest that the conserved PilC/PilY1 β-propellor domain accelerates or stabilizes formation of the tip initiation holocomplex. Like the conserved C-terminal β-propellor of PilC/Y1, the platform of some T2SS substrates, including cholera toxin and *E. coli* heat labile toxin, have β-propellor folds. However,

these secreted proteins do not require strand complementation on PilK for association with the tip complex. This is consistent both with a conserved role for the β-propellor in fiber initiation or extension, and with the requirement for T2SS payloads to be released from the extended pseudopilus rather than stably retained at the fiber tip. The β-propellor may accelerate or stabilize assembly of the tip complex, promote gating of the secretin pore (Guo et al. 2024), or both. However, neither the β-propellor nor the C-terminal β-strand are formally essential for fiber initiation, since strains lacking PilC/PilY1 or core minor pilins, are piliated when retraction is prevented by removal of the PilT retraction ATPase. The idea that PilC/PilY1 promote assembly of minor pilins in the tip complex is strongly supported by observations that pili which assemble in the absence of both PilC/PilY1 and the retraction ATPase PilT are depleted of tip-associated minor pilins (Hanne C. Winther-Larsen et al. 2005).

Bioinformatic analyses of T4F systems have provided a roadmap of evolutionary trajectories for diverse T4F (Denise et al. 2019). AlphaFold modeling provides a remarkable platform for predicting how tip complexes have diverged over time and across ecological niches. Our models of diverse T4F suggest the MSHA protein MshQ may act as a functional homolog of PilC/PilY1 proteins (**Fig. 3-S9**). Viewed in the context of T4F phylogenies, these models suggest that PilC/PilY1 and other large adhesins evolved after the divergence of Com T4dP from the ancestor of modern T4aP/T2SS/MSHA pili. However, the absence of a functional homolog in T4aP required for DNA uptake from *V. cholerae*, and in T2SS which fall within this clade, may suggest that tip adhesins were subsequently lost from certain lineages (**Fig. 3-S9**).

In solved structures of T4bP tip complexes from the *V. cholereae* toxin co-regulated pilus (TCP) and the colonization factor antigen/III (CFA/III) pilus found in human enterotoxigenic *E. coli*, the filament tip is composed of a minor pilin homotrimer with fundamentally distinct

pilin-pilin interactions (Kawahara et al. 2016). These T4P gene loci only contain a single minor pilin gene, in contrast with most T4F systems which harbor multiple minor pilins, encoded within syntenic operons. But some T4bP operons do encode PilIJK homologs, including the bundle-forming pili (BFP) found in some *E. coli* lineages, Together, these observations suggest that the ancestral T4bP diverged from other T4F tip complex assembly mechanisms early in evolution, consistent with phylogeny-based predictions (**Fig. 3-S8**) (Denise et al. 2019). This interpretation is strengthened when we examine T4cP and T4dP.

T4dP Com (competence) pili are unique to Gram-positive bacteria. For *Streptococcus* spp., modeling and experiments support the formation of a tip complex containing PilIJK homologs ComGE/GF/GG (Ng et al. 2016; Jeremy Mom et al. 2024). ComGF is needed for DNA binding (Ng et al. 2016; Gu et al. 2021; Kellogg et al. 1963). Similarly, the *B. subtilis* Com operon comprises ComGE/GF/GG proteins. As in *S. pneumoniae*, *B. subtilis* ComGF contains a canonical prepilin signal sequence. Our AlphaFold modeling confidently predicts the formation of a *B. subtilis* tip complex. However, processed *B. subtilis* ComGF lacks the typical pilin N-terminal domain. Our *B. subtilis* model (**Fig. 3-S9**) confidently predicts that the extreme C-terminal β-strand of ComGG behaves similarly to the T2SS GspK homolog, Curiously, however, the *S. pneumoniae* ComGG was previously modeled with low confidence as an α-helix, not a β-strand (Ng et al. 2016; Jeremy Mom et al. 2024). Nevertheless, ComGF interacts with GE and GG in the same orientation in models of both *Streptococcus* and *B. subtilis* tip complexes. Thus, it appears likely that β-strand complementation occurs in at least part of the Com T4dP clade (**Fig. 3-S8, S9**). Similarly, our modeling and experiments show that the minor pilin-like protein CpaL from Tad T4cP systems acts as a PilK analog (**Fig. 3-S1, Fig. 3-5**) (Grünwald et al. 2008). In summary, β-strand complementation in PilK paralogs may

occur, *in cis* or *in trans*, in T2SS, T4aP, T4bP, T4cP, and T4dP. We therefore suggest that licensing mechanisms like those characterized here are common to many or even most T4F systems, and that these mechanisms arose early in the evolution of T4F.

3.6 Materials & Methods

3.6.1 Bacterial strains and culture conditions.

Neisseria gonorrhoeae strain FA1090, *Acinetobacter baylyi* strain ADP1, and the hyperpiliated derivative *Caulobacter crescentus* CB13 strain bNY30a were used in this study. For a list of strains, see **Table 3-S1**. *N. gonorrhoeae* was grown on GCB agar with Kellogg's supplements (Kellogg et al. 1963). *A. baylyi* cultures were grown at 30 °C in Miller lysogeny broth (LB) medium and on agar supplemented with kanamycin (50 μg/ml), spectinomycin (60 μg/ml), zeocin (50 μg/ml), and apramycin (50 μg/ml) where appropriate. *C. crescentus* was grown in peptone yeast extract (PYE) medium and on agar supplemented with kanamycin (5-10 μg/ml) and nalidixic acid (20 μg/ml) where appropriate.

3.6.2 Strain construction

N. gonorrhoeae

Mutations were introduced in the FA1090 background by spot transformations of PCR products and/or linearized plasmids. Transformed spots were streaked to GCB plates or GCB plates with the appropriate antibiotic then colonies were screened by sequencing of the mutated locus.

To construct the pilE-T125C strains AMN64 and AMN65, pilE(1-81-S2) was amplified and mutated to T125C by overlap extension PCR. To disrupt pilT in the pilE-T125C

background, the ΔpilT::ermC allele was amplified directly from AMN4 and used to transform AMN65. All other mutations were introduced by transformation of plasmids constructed by Gibson assembly of PCR products, gBlocks (IDT) and/or extended oligonucleotides into pBluescript KS(+).

For transformation assays pAMP2097was prepared. This plasmid contains the gyrB-D429N allele, which confers resistance to nalidixic acid, and a *Neisseria* DNA uptake sequence. *N. gonorrhoeae* AMN18 genomic DNA was used as template for PCR with primers MS11_gyrB-F and MS11_gyrB-R. The PCR product was purified, digested with EcoRI and ClaI (NEB) and cloned into pBluescriptKS+ (Stratagene), yielding AMP2096. Site-directed mutagenesis of AMP2096 with primers gyrB_D429N-f and gyrB_D429N-r was used to introduce the D429N mutation, resulting in pAMP2097.

C. crescentus

In-frame deletion strains were constructed by double homologous recombination using pNPTS-derived plasmids as previously described. S-17 *E. coli* cells harboring pNPTS-derived plasmids were grown to exponential phase and then 100 µl was pelleted by centrifugation at 18,000*g* for 1 min. One ml of overnight culture of *C. crescentus* was pelleted by centrifugation at 5,200*g* for 1 min, and then both pellets were resuspended in the same 10 µl of fresh PYE and spotted onto a PYE 1.5% agarose plate. Plates were incubated overnight at 30 °C, and the next day cells were removed from the plate and resuspended in 100 µl PYE before plating on PYE plates containing kanamycin and nalidixic acid. After three days of growth at 30 °C, colonies were patched onto fresh kan/nal PYE plates and grown overnight at 30 °C. The next day, cells from each patched colony were inoculated into 3 ml PYE medium and grown overnight at 30 °C.

10 µl of overnight culture was then spotted onto PYE plates containing 3% sucrose and struck out for single colony isolation. Sucrose plates were grown for three days at 30 °C and then 4-6 colonies from each plate were patched onto PYE plates +/- kanamycin and incubated overnight at 30 °C. Colonies that were kanamycin sensitive were confirmed by PCR and nanopore sequencing using primers.

For construction of the pNPTS-derived plasmids, ~500 bp flanking regions of DNA on either side of the desired mutations were amplified from bNY30a DNA. Upstream regions were amplified using F1 and R1 primers while downstream regions were amplified using F2 and R2 primers. The resulting amplified DNA was purified (Qiaquick) and assembled into pNPTS138 that had been digested with restriction enzyme *Eco*RV (New England Biolabs) using HiFi Assembly Master Mix (New England Biolabs).

3.6.3 Modeling

Preliminary modeling was done using AlphaFold2 in the CollabFold environment (Mirdita et al. 2022). The modeling shown in the figures was done using AlphaFold3 (Abramson et al. 2024) on the DeepMind server. Protein processing sites were predicted through a combination of manual analysis, freely available prediction software SignalP 6.0, and/or DeepTMHMM (Teufel et al. 2022).

3.6.4 Minor pilin expression in *E. coli*

Minor pilin proteins were produced in soluble form with oxidized disulfide bonds in the *E. coli* periplasm as described (Applegate et al. 2026). Size exclusion chromatography was done on a calibrated Superdex 75 Increase 10/300 column (Cytiva). For co-expression of soluble PilK-His_6 and PilC, PilK-His_6 was expressed from a plasmid previously described (Applegate et

al., 2026), and FLAG-PilC(533-1060) bearing an N-terminal signal peptide was expressed from a low-copy plasmid pmr101A.

Expression vectors encoding PilK-His_6 and FLAG-PilC(533-1060) were co-transformed into competent *E. coli* BL21(DE3) cells. A single colony was picked and added to LB medium supplemented with 100 µg/ml ampicillin and 50 µg/ml kanamycin. This culture was grown overnight shaking at 200 rpm at 37° C. 5 mL of seed culture was added to a 2 L baffled flask containing 1 L ZYM-5052 (Studier 2005), supplemented with 100 µg/ml ampicillin and 50 µg/ml kanamycin, then grown at 37° C, shaking at 200 rpm. When cells reached an optical density at 600 nm of 1.0, they were moved to a 16° C incubator and shaken at 200 rpm. Cultures were grown for an additional 18 hours before being harvested by centrifuging at 4670 x g for 15 min and 4° C (Sorvall H6000A, RC-3B Refrigerated Centrifuge).

Purification was performed *via* periplasmic fractionation and Ni^{2+}-NTA sepharose HP (Cytiva) metal affinity purification as described in Applegate et al. (2026).

For immunoblotting, samples were mixed with 4x Laemmli buffer containing 20% 2-mercapto-ethanol (5% v/v final) then incubated at 95° C for 5 minutes. Samples were loaded into 12.5% (w/v) SDS-PAGE gels and run for 60 minutes at 190 V. Gels were either transferred to a 0.45 µm nitrocellulose membrane (Schleicher & Schuell BA85). Membranes were blocked with PBS Blocking Buffer (LICORbio) for 1 hr at room temperature then incubated with primary antibody (ANTI-FLAG M2 antibody, Sigma-Aldrich F3165) for 1 hour at room temperature. The membrane was rinsed in PBST 5 times for 5 minutes before being incubated with secondary antibody diluted 1:10,000 (Goat anti-Mouse IgG H+L Highly Cross-Adsorbed Secondary Antibody Alexa Fluor 488, Invitrogen A32723TR) for 45 minutes at RT. Membrane was then

rinsed in PBST 5 times for 5 minutes and imaged using an Odyssey imaging system (LI-COR Biotech).

3.6.5 Live cell imaging and in vivo labeling of dynamic T4P

N. gonorrhoeae

Pilus labeling was as described (Kraus-Römer et al., 2022), with modifications. Briefly, *N. gonorrhoeae* cells expressing Cys-substituted PilE major pilin were grown on GCB agar with Kellogg supplements and resuspended into Labeling Medium: DMEM (FluoroBrite, Gibco A18967-01) that had been supplemented with 1× GlutaMAX (Gibco 35050-061) and 30 mM HEPES, and pre-equilibrated to 37°C and 5% CO_2. The cell suspension was adjusted to OD_{600nm} ~0.2 in 1mL, in 1.8 mL round-bottom microcentrifuge tubes. The cells were sedimented (7,000rpm, 1 min.) and resuspended in Labeling Medium containing 20 µM Alexa Fluor 488 C5 Maleimide (Thermo-Fisher #A10254, FW=721), from a 5 mM stock solution prepared in anhydrous DMSO. The cells were incubated at 37°C and 5% CO_2 with periodic gentle swirling of the cells for 15min. The labeled cells were sedimented (7,000 rpm, 1 min.), washed in 1 mL of Labeling Medium, again sedimented, and washed for a total of three times before finally being resuspended in 200 µL of Imaging Medium: Labeling Medium, further supplemented with 500 µM TEMPOL (Enzo #ALX-431-081G001), 1 mM Trolox (Vector Labs CB-01000-2), 500 µM freshly prepared ascorbic acid, and 0.3% bovine serum albumin. For some samples, wells were additionally pre-treated with 0.01% poly-L-lysine to stick bacteria to the coverslip. T4P were observed using a Yokogawa CSU-X1 spinning disk confocal head, with a 100X/1.45 NA Plan Apochromat objective. For excitation a 488 nm diode laser was coupled to the confocal head using a single mode fiber. The incident illumination power was calibrated at the objective back

aperture using a laser power meter (Thorlabs) and corresponded to 15-20 W/cm^2 at the sample plane (Grünwald et al., 2008). Image sequences were captured using an Andor 888 EMCCD camera operated at 25 frames/s. The microscope system was controlled, and data were acquired, using NIS Elements software.

A. baylyi

Pilin labeling in *A. baylyi* was performed as described previously (C. K. Ellison et al. 2017; C. K. Ellison, Dalia, et al. 2019). Briefly, 100 µL of overnight cultures was added to 900 µL of fresh LB in a 1.5 mL microcentrifuge tube, and cells were grown at 30 °C rotating on a roller drum for 70 min. Cells were then centrifuged at 18,000*g* for 1 min and resuspended in 50 µL of LB before labeling with 25 µg/mL of AlexaFluor488 C5-maleimide (AF488-mal) (ThermoFisher) for 15 min at room temperature. Labeled cells were centrifuged, washed three times with 100 µL of PBS and resuspended in 5–20 µL PBS. Cell bodies were imaged using phase-contrast microscopy while labeled pili were imaged using fluorescence microscopy on a Nikon Ti2-E microscope using a Plan Apo 100X oil immersion objective, a GFP/FITC/Cy2 filter set for pili, a Hamamatsu ORCA-Fusion Gen-III cCMOS camera, and Nikon NIS Elements Imaging Software. Cell numbers and the percent of cells making pili were quantified manually using Fiji. All imaging was performed under 1% agarose pads made with PBS solution.

C. crescentus

Pilin labeling was performed the same as *A. baylyi* with some differences. 500 µl of overnight cultures grown in 3 ml of PYE at 30 °C was diluted into 3 ml fresh PYE and grown for 5 hr at 30 °C. 200 µl was then pelleted at 5,200*g* and resuspended in 50 µl PYE and labeled with 25 µg/mL of AlexaFluor488 C5-maleimide (AF488-mal) (ThermoFisher) for 25 min at room

temperature. Labeled cells were centrifuged, washed three times with 100 µL of PYE and resuspended in 5–20 µL PYE.

The percentage of cells expressing T4P for all species was manually quantified using Fiji software. Micrograph images of T4P were analyzed using Nikon NIS Elements software and ImageJ. Micrographs are representative of each strain and are presented with intensity equalized over time, as well as a rolling median over every 3 frames to minimize background noise. The LUTs for *N. gonorrhoeae* strains were adjusted for each strain to optimize visualization of T4P present. For *A. baylyi* and *C. crescentus*, LUTs were normalized for each species.

3.6.6 Transformation assays

N. gonorrhoeae

Cells were grown on GCB agar with Kellogg supplements and resuspended into 500 µL GCBL media supplemented with 5 mM $MgSO_4$. Cell suspensions were adjusted to $1.2x10^7$ cfu/ml. Suspensions were then incubated with 250ng linearized AMP2097 for 15min at 37˚ C 5% CO_2 in a 96-well plate format (Falcon #351172). The transformation mixture was then diluted 1:10 into GCBL media supplemented with Kellogg supplements and incubated for 4 hours at 37 ˚C 5% CO_2. Subsequent 1:10 serial dilutions of the transformation reaction mix were performed into GCBL media supplemented with Kellogg supplements. The serial dilutions were plated using the "dribble plating" method described previously onto 2 sets of plates: GCB plates and plates containing GCB supplemented with 1.5 µg/ml Nalidixic acid (both supplemented with Kellogg supplements). Plates were left to grow for two nights at 37˚C 5% CO_2 before assessing colony growth. For quantitative transformation in the presence of IPTG, cells were grown on GCB agar supplemented with 1 mM IPTG on the surface of the agar. Subsequent GCBL media

used for resuspension, transformation, and serial dilutions were also supplemented with 1 mM IPTG. Plates used for dribble plating did not contain IPTG.

Movie analysis was performed with videos of AMN64 and AMN70 taken under identical conditions. The LUTs were set to the same range. Videos have their intensities equalized over time and are portrayed as a rolling median over 3 frames.

3.7 Acknowledgements

We thank K. Forest, H. Seifert, and R. Klevit for helpful discussions, D. Miller for suggesting the term “licensing,” and M. So and H. Seifert for sharing materials. This work was funded by R21 AI155991 (AJM), R35 GM150916 (CE), T32AI07410 (JA), T32GM153507 (ZRL), University of Washington School of Medicine Molecular Biophysics Training Program Hurd Fellowship (ZRL), University of Washington School of Medicine Medical Scientist Training Program (T32 GM007266 and T32 GM153182) and the University of Washington Bacterial Research Fund, including a gift from Dr. J.M. Griffiss (SM, AJM). Courtney Ellison, PhD, is a Damon Runyon-Marilyn and Scott Urdang Breakthrough Scientist supported by the Damon Runyon Cancer Research Foundation (DFS6023)

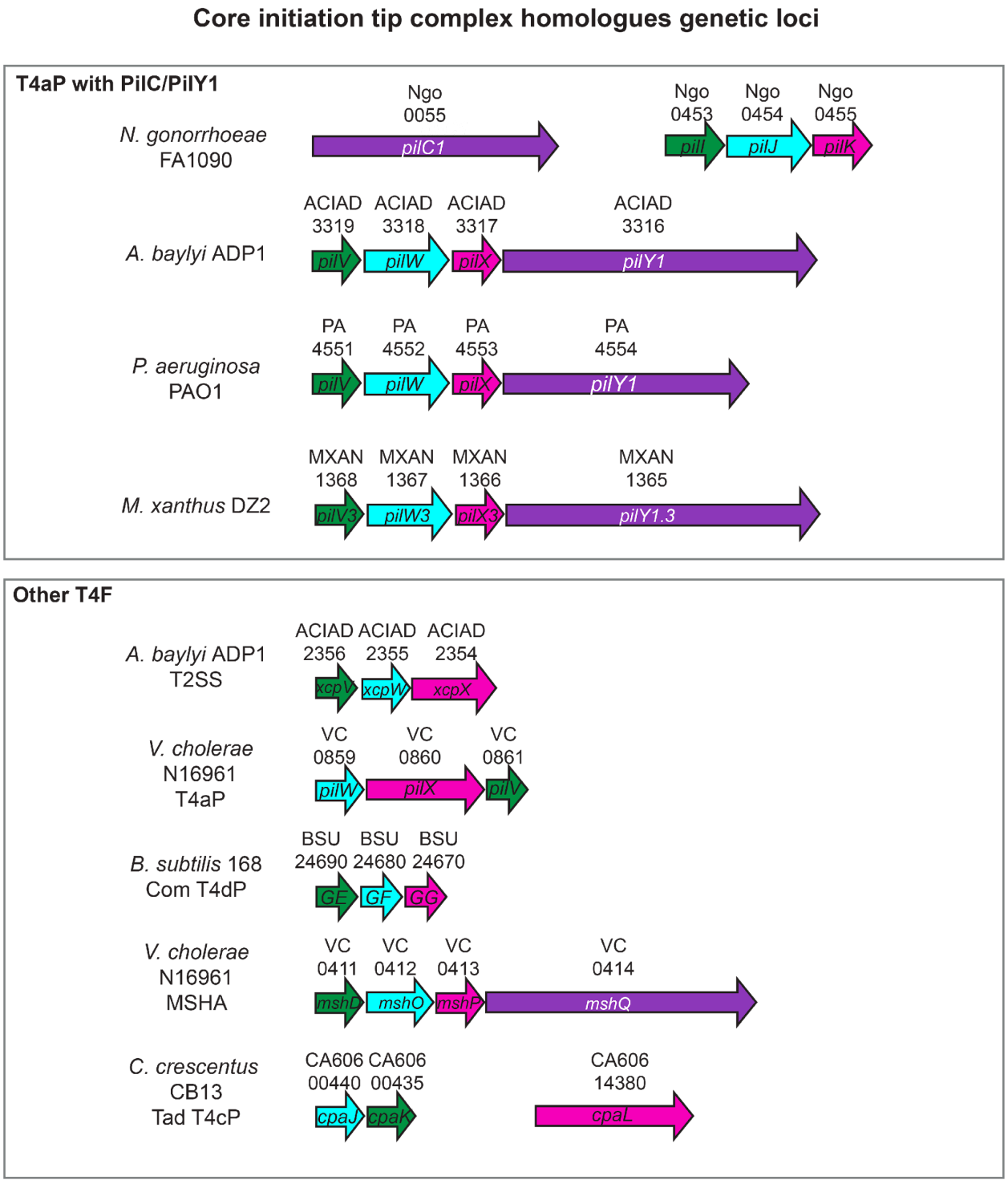

Figure 3-S1. Schematic of genetic loci for several T4F discussed in this chapter.
Numbers above genes indicate locus tags. Protein homologues are colored correspondingly.

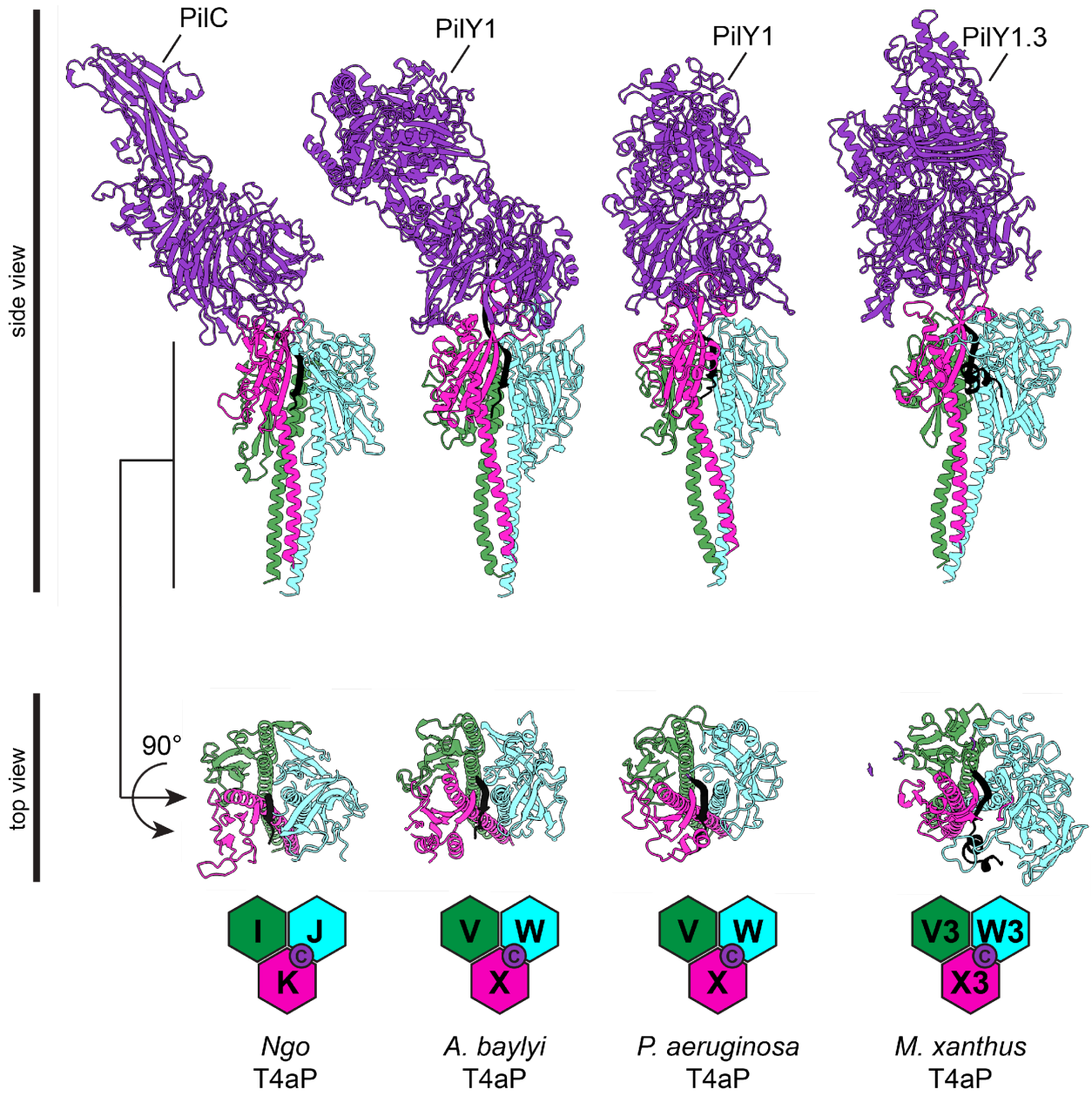

Figure 3-S2. A β-strand at the extreme C-terminus of PilC/PilY1 adhesins is predicted to act *in trans* to complete the β-sheet of minor pilin PilK homologs in T4aP.
AlphaFold models are shown for minor pilin heterotrimers in complex with PilC or PilY1. In each model, the C-terminal β-strand is colored black.

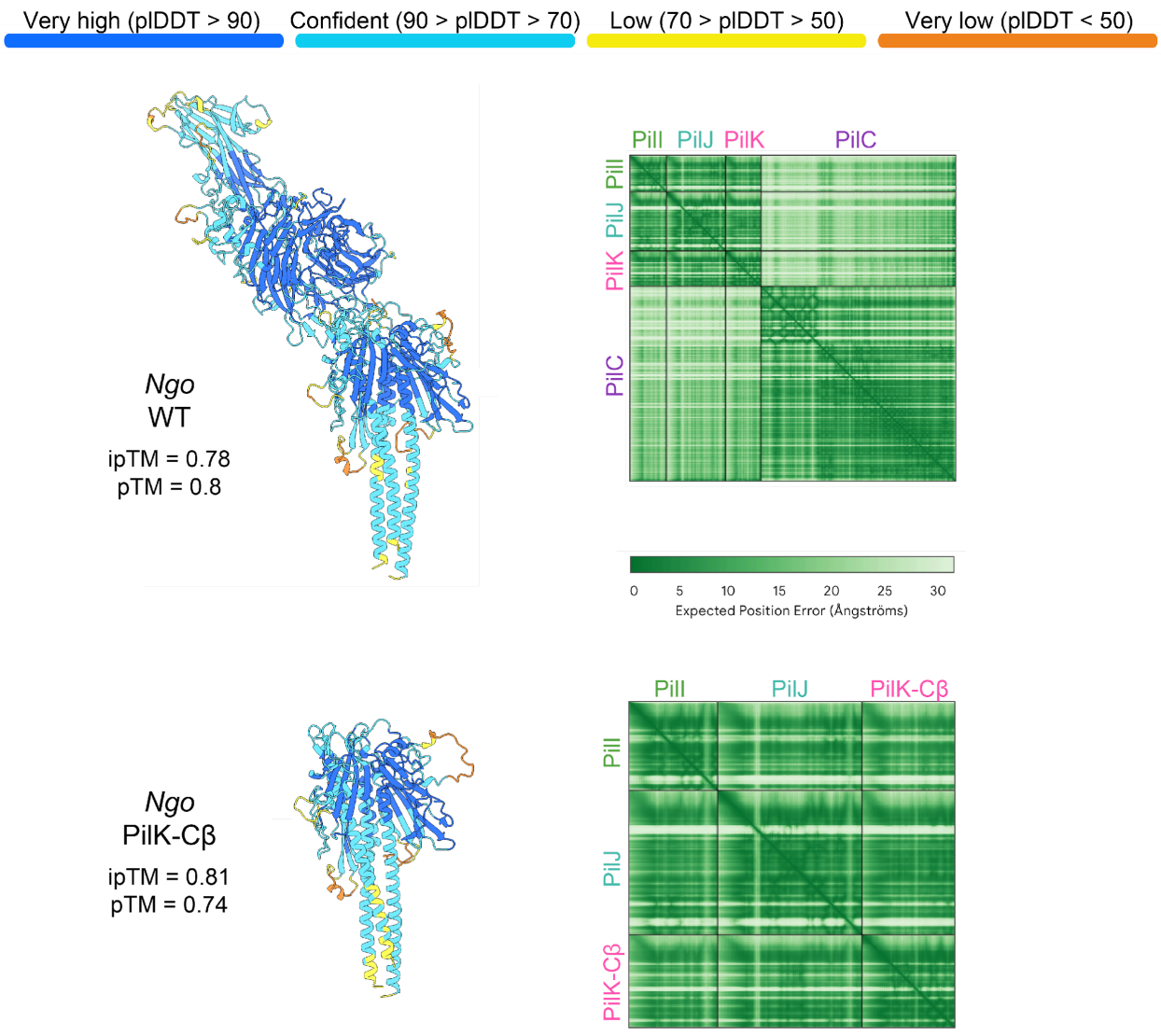

Figure 3-S3. AlphaFold confidence metrics for tip complexes from wildtype *N. gonorrhoeae* (PilI/J/K/C, top) and a complex with the PilK-Cβ chimeric protein used in this work (PilI/J/K-Cβ, bottom) . Structures on the left are colored by confidence intervals indicated at the top. The boxes on the right show predicted aligned error of structures on the left.

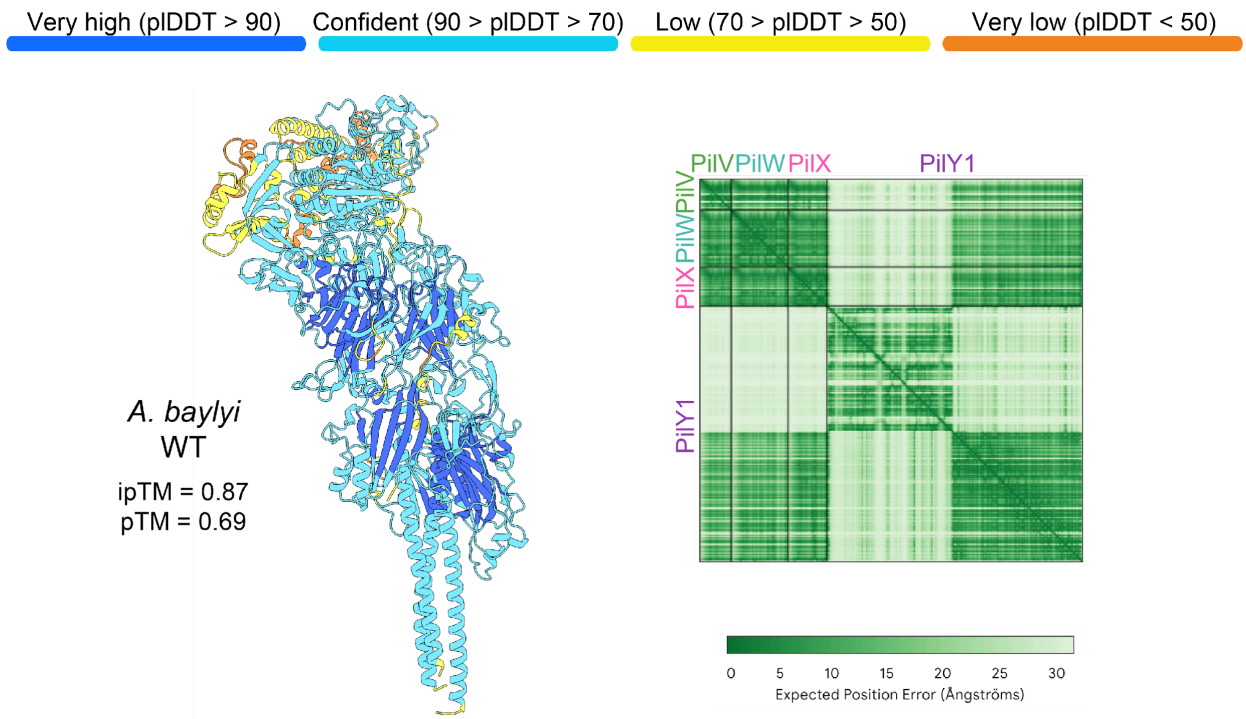

Figure 3-S4. AlphaFold confidence metrics for the tip complex from wildtype *A. baylyi.* Structure on the left is colored by confidence intervals indicated at the top. The box on the right shows the predicted aligned error of structure on the left.

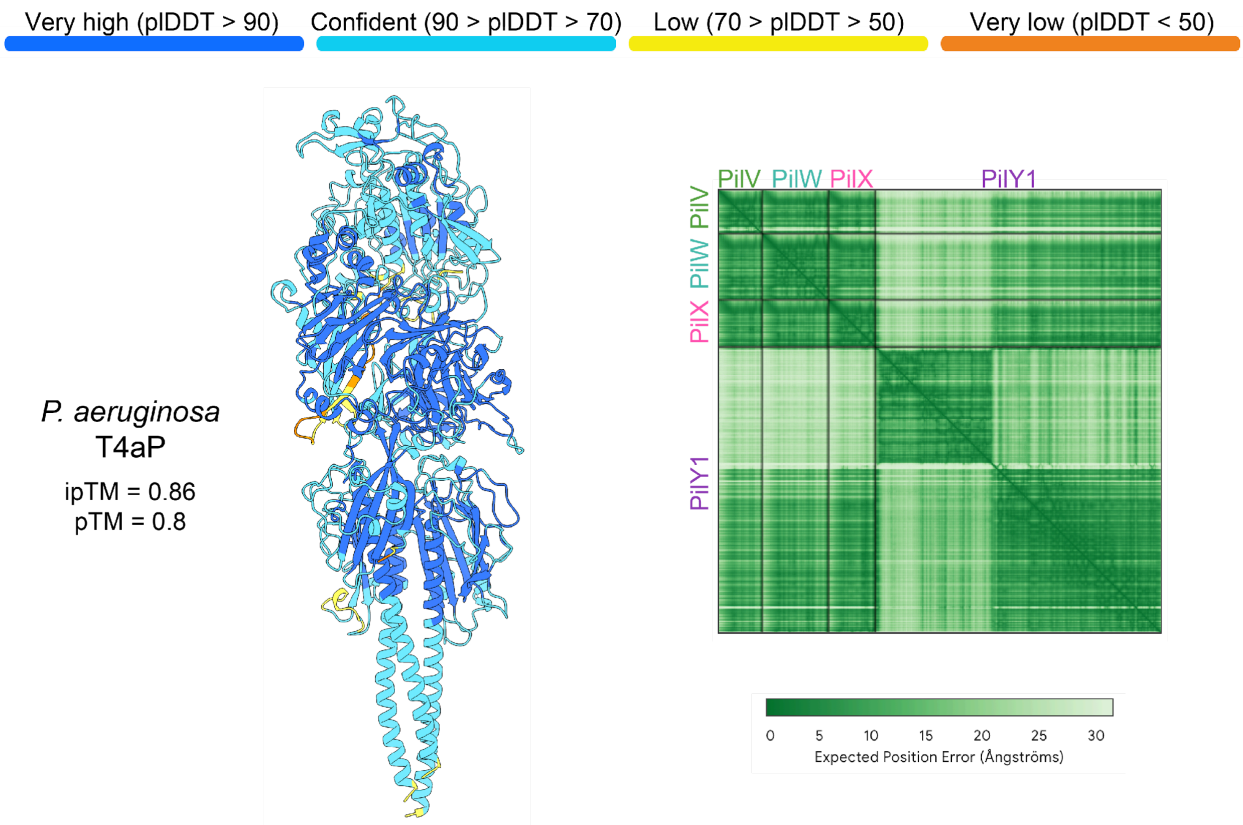

Figure 3-S5. AlphaFold confidence metrics for the tip complex from wildtype *P. aeruginosa* Structure on the left is colored by confidence intervals indicated at the top. The box on the right shows the predicted aligned error of structure on the left.

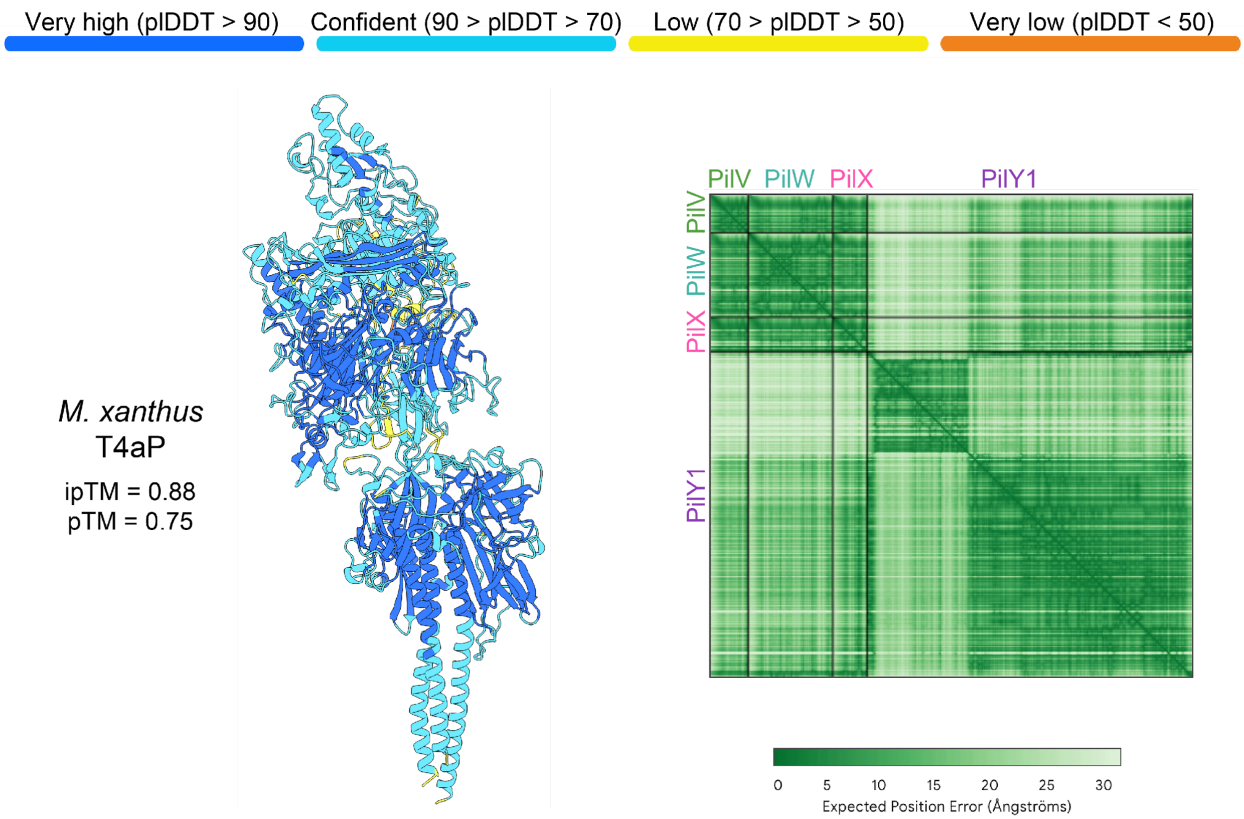

Figure 3-S6. AlphaFold confidence metrics for the tip complex from wildtype *M. xanthus*. Structure on the left is colored by confidence intervals indicated at the top. The box on the right shows the predicted aligned error of structure on the left.

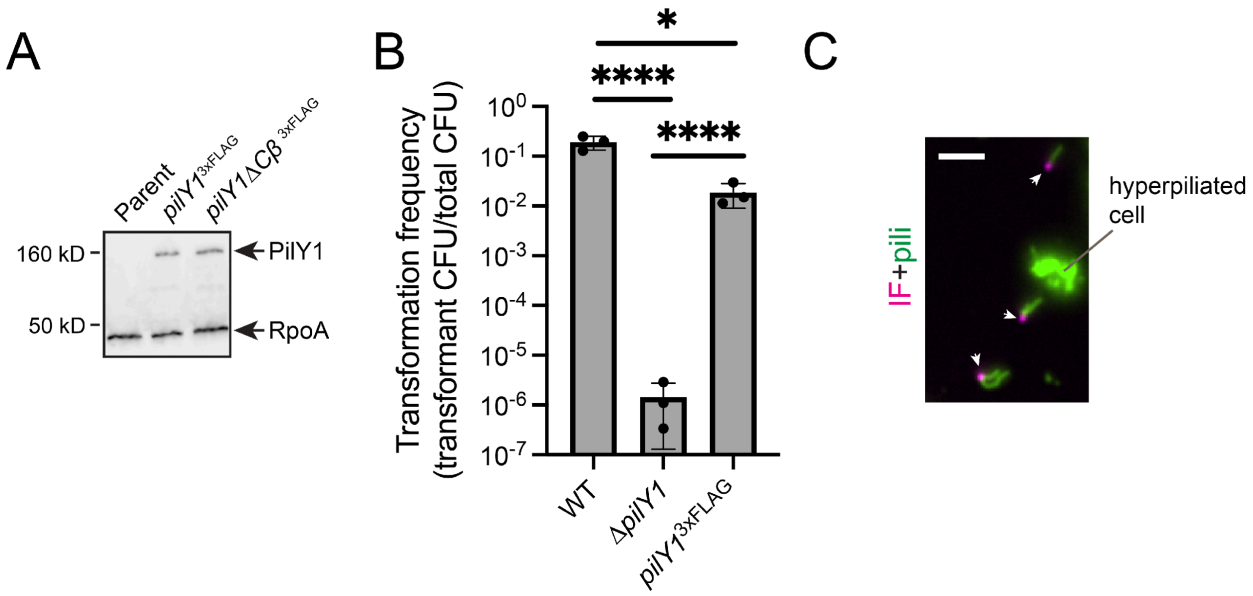

Figure 3-S7. PilY1^{3xFLAG} and immunofluorescence supplementary data.
(A) Representative Western analysis of indicated strains. RpoA was used as a loading control. Blot was probed with both α-FLAG and α-RpoA antibodies. (B) Natural transformation assay data from indicated strains. Bar graph shows the mean +/- SD. Each dot represents an independent, biological replicate. Statistical analysis for natural transformation assays was performed on log-transformed transformation frequency data. Statistics were determined by Sidak's multiple comparisons test. ****P<0.0001; *P<0.05. (C) Representative microscopy image of sheared T4P with tip-associated PilY1 signal. White arrows indicate examples of PilY1 localized to the tips of sheared T4P filaments. Scale bar, 2 μm.

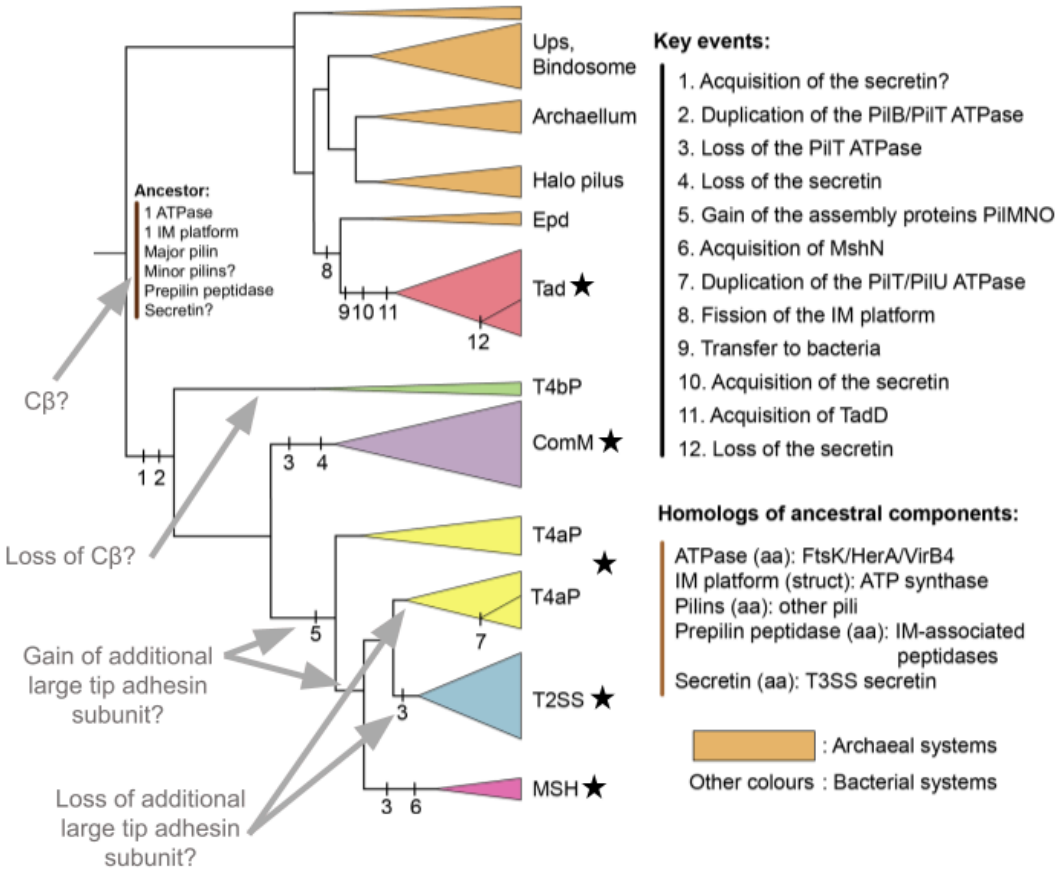

Figure 3-S8. Phylogenetic tree showing the evolutionary relatedness between different types of T4F.

(Previously published Figure 7 from Denise et al. 2019) Black stars (★) were added here to indicate clades with evidence of β-strand complementation as a mechanism for tip complex licensing. Gray arrows and gray text were added here to indicate potential evolutionary trajectories of tip complex components and aid in discussion.

Modified from Denise et al. 2019 Figure 7 legend:

The tree was based on the information of the trees of the concatenate and simplified to highlight the key clades and events. The colour of the triangles indicates the type of the systems. Each vertical bar on the branch indicates a numbered evolutionary event, whose details are specified under the corresponding number in the list 'Key events'. The hypotheses for the composition of the last common ancestor of the T4F superfamily are indicated at the root, and the distant homologues of these systems are indicated in the list 'Homologous of ancestral components', in which homology was observed by sequence ('aa') or structural ('struct') similarity. Halo pilus indicates two pili characterised in Halobacteria. Aap, adhesive archaeal pilus; Epd, EppA dependent; IM, integral membrane; MSH, mannose-sensitive hemagglutinin pilus; Tad, tight adherence; T4F, type IV filament; T2SS, type II protein secretion system; T3SS, type III protein secretion system; T4aP, type IVa pilus; T4bP, type IVb pilus; Ups, UV-inducible pilus of *Sulfolobus*.

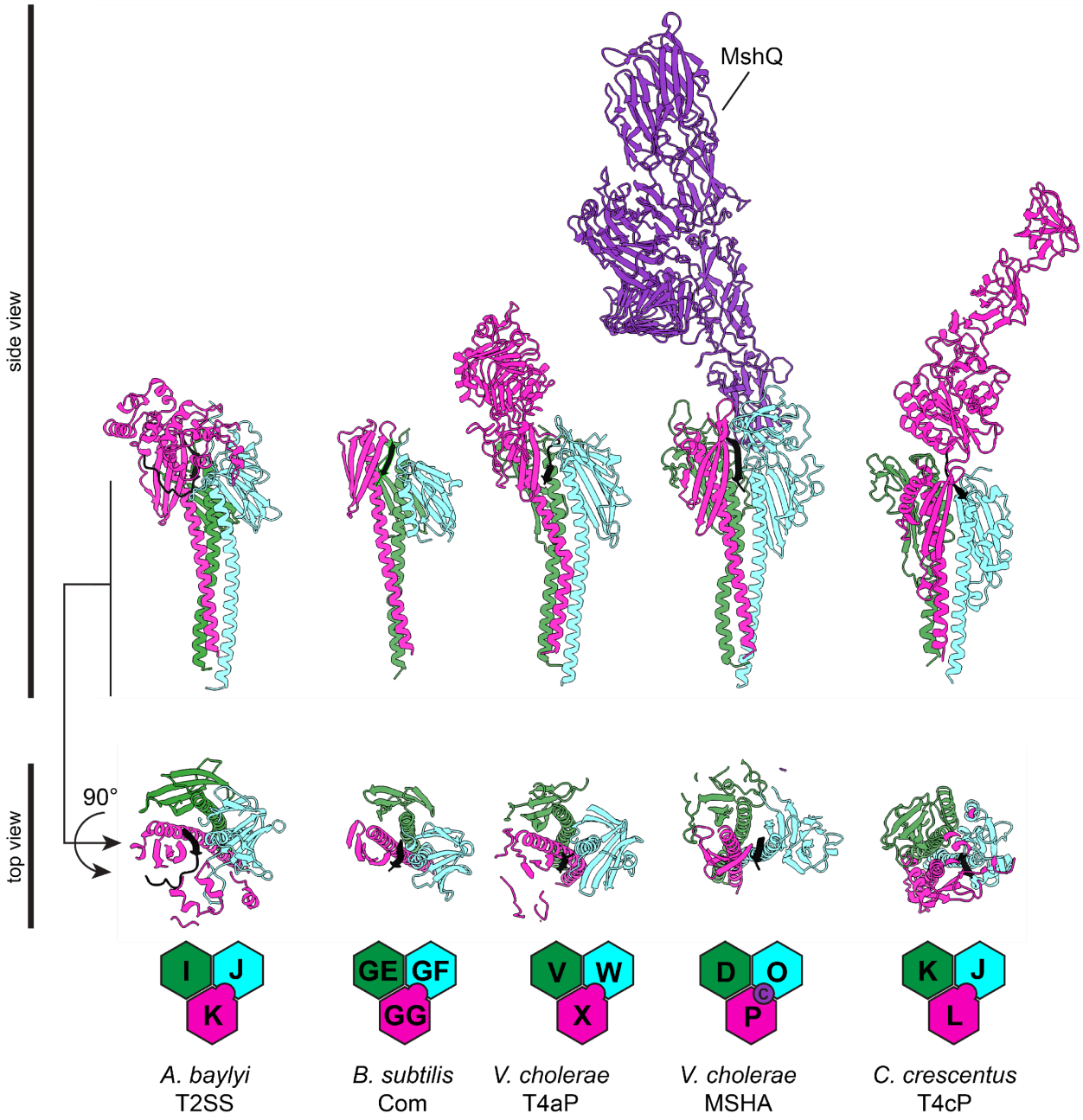

Figure 3-S9. A conserved β-strand is predicted to strand-complement the β-sheet in GspK homologues of diverse T4F

AlphaFold-predicted models of predicted tip complexes for indicated species. In all models, the conserved C-terminal β-strand is colored black.

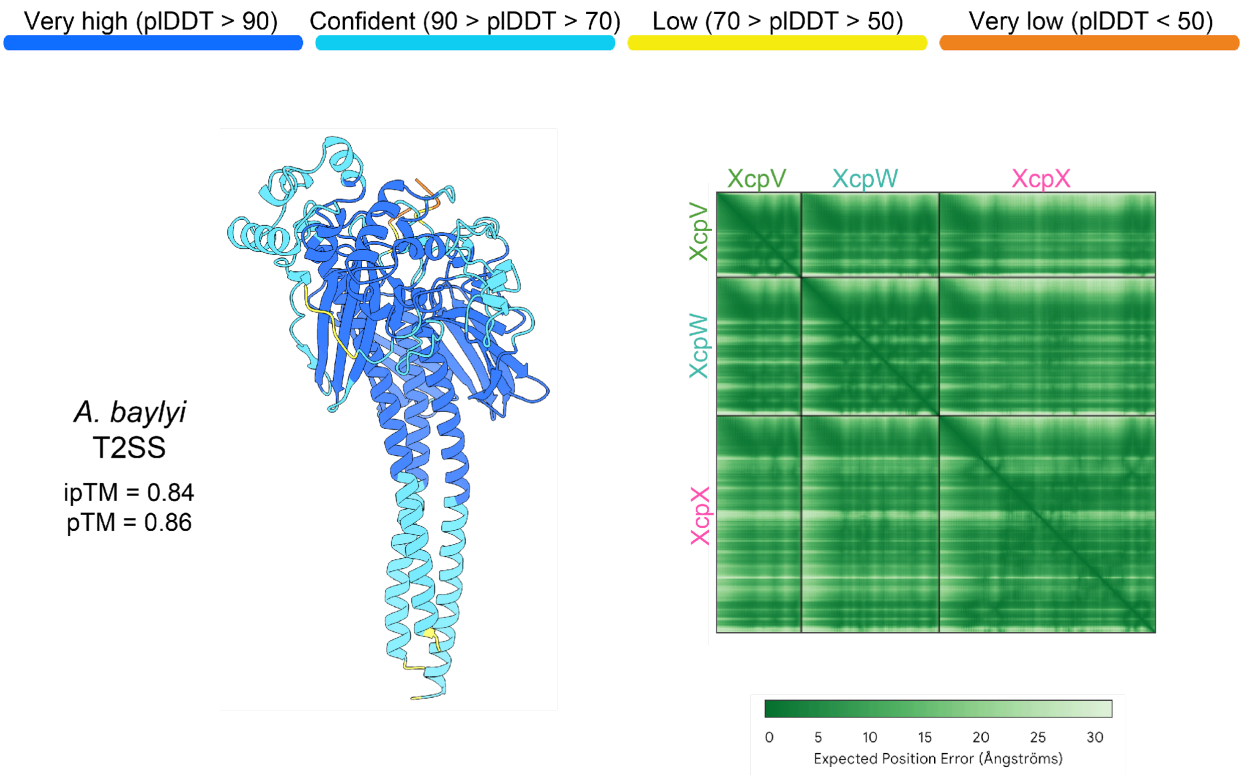

Figure 3-S10. AlphaFold confidence metrics for the tip complex from the T2SS in *A. baylyi*. Structure on the left is colored by confidence intervals indicated at the top. The box on the right shows the predicted aligned error of structure on the left.

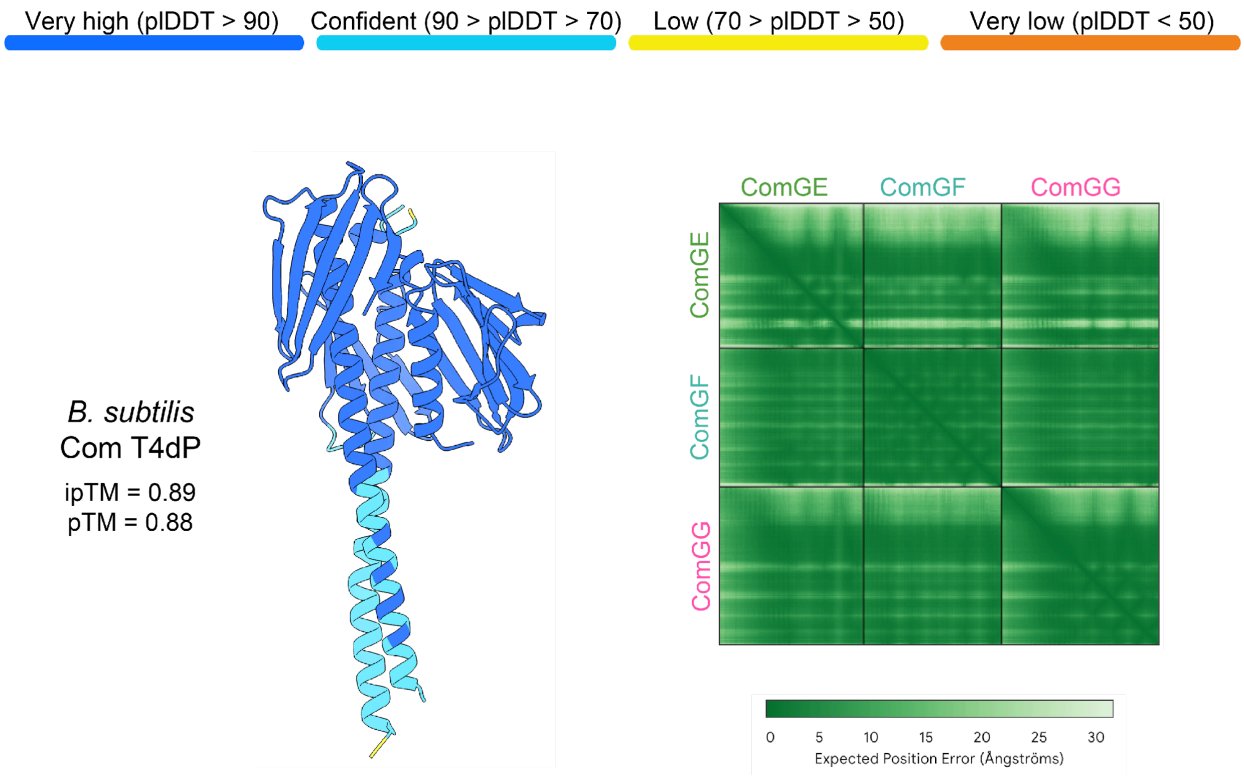

Figure 3-S11. AlphaFold confidence metrics for the tip complex from the Com pilus in *B. subtilis*.
Structure on the left is colored by confidence intervals indicated at the top. The box on the right shows the predicted aligned error of structure on the left.

Chapter 4. References

Aas, Finn Erik, Cecilia Løvold, and Michael Koomey. 2002. “An Inhibitor of DNA Binding and Uptake Events Dictates the Proficiency of Genetic Transformation in Neisseria Gonorrhoeae: Mechanism of Action and Links to Type IV Pilus Expression.” *Molecular Microbiology* 46 (5): 1441–50. https://doi.org/10.1046/j.1365-2958.2002.03265.x.

Abramson, Josh, Jonas Adler, Jack Dunger, et al. 2024. “Accurate Structure Prediction of Biomolecular Interactions with AlphaFold 3.” *Nature* 630 (8016): 493–500. https://doi.org/10.1038/s41586-024-07487-w.

Alm, R. A., J. P. Hallinan, A. A. Watson, and J. S. Mattick. 1996. “Fimbrial Biogenesis Genes of Pseudomonas Aeruginosa: pilW and pilX Increase the Similarity of Type 4 Fimbriae to the GSP Protein-Secretion Systems and pilY1 Encodes a Gonococcal PilC Homologue.” *Molecular Microbiology* 22 (1): 161–73. https://doi.org/10.1111/j.1365-2958.1996.tb02665.x.

Almagro Armenteros, José Juan, Konstantinos D. Tsirigos, Casper Kaae Sønderby, et al. 2019. “SignalP 5.0 Improves Signal Peptide Predictions Using Deep Neural Networks.” *Nature Biotechnology* 37 (4): 420–23. https://doi.org/10.1038/s41587-019-0036-z.

Applegate, Justin, Emma Miller, Zoey Litt, et al. 2026. “Expression of Soluble Type IV Minor Pilins and Isolation of a Neisseria Gonorrhoeae PilI-PilJ Subcomplex.” *bioRxiv*, January 1, 2026.02.09.704877. https://doi.org/10.64898/2026.02.09.704877.

Barnier, Jean-Philippe, Julie Meyer, Subramania Kolappan, et al. 2021. “The Minor Pilin PilV Provides a Conserved Adhesion Site throughout the Antigenically Variable Meningococcal Type IV Pilus.” *Proceedings of the National Academy of Sciences* 118 (45): e2109364118. https://doi.org/10.1073/pnas.2109364118.

Berry, Jamie-Lee, and Vladimir Pelicic. 2015. “Exceptionally Widespread Nanomachines Composed of Type IV Pilins: The Prokaryotic Swiss Army Knives.” *FEMS Microbiology Reviews* 39 (1): 134–54. https://doi.org/10.1093/femsre/fuu001.

Boslego, John W., Edmund C. Tramont, Raymond C. Chung, et al. 1991. “Efficacy Trial of a Parenteral Gonococcal Pilus Vaccine in Men.” *Vaccine* 9 (3): 154–62. https://doi.org/10.1016/0264-410X(91)90147-X.

Bradley, D. E. 1974. “The Adsorption of Pseudomonas Aeruginosa Pilus-Dependent Bacteriophages to a Host Mutant with Nonretractile Pili.” *Virology* 58 (1): 149–63. https://doi.org/10.1016/0042-6822(74)90150-0.

Brinton, C., J. Bryan, J. Dillon, et al. 1978. “Uses of Pili in Gonorrhea Control Role of Bacterial Pili in Disease Purification and Properties of Gonococcal Pili and Progress in the Development of a Gonococcal Pilus Vaccine for Gonorrhea.” July 28.

https://www.semanticscholar.org/paper/Uses-of-pili-in-gonorrhea-control-role-of-bacterial-Brinton-Bryan/ef7aba5ceb3bd9916d976cf9028d07ec68f8509e.

CDC. 2025. “Sexually Transmitted Infections Surveillance, 2024.” STI Statistics. https://www.cdc.gov/sti-statistics/annual/index.html.

CDC. 2026. “CDC Acts on Presidential Memorandum to Update Childhood Immunization Schedule.” CDC Newsroom, January 5. https://www.cdc.gov/media/releases/2026/2026-cdc-acts-on-presidential-memorandum-to-update-childhood-immunization-schedule.html.

Charles-Orszag, Arthur, Marleen van Wolferen, Samuel J. Lord, Sonja-Verena Albers, and R. Dyche Mullins. 2024. “Adhesion Pilus Retraction Powers Twitching Motility in the Thermoacidophilic Crenarchaeon Sulfolobus Acidocaldarius.” *Nature Communications* 15 (1): 5051. https://doi.org/10.1038/s41467-024-49101-7.

Craig, Lisa, Katrina T. Forest, and Berenike Maier. 2019. “Type IV Pili: Dynamics, Biophysics and Functional Consequences.” *Nature Reviews. Microbiology* 17 (7): 429–40. https://doi.org/10.1038/s41579-019-0195-4.

Craig, Lisa, Ronald K. Taylor, Michael E. Pique, et al. 2003. “Type IV Pilin Structure and Assembly: X-Ray and EM Analyses of Vibrio Cholerae Toxin-Coregulated Pilus and Pseudomonas Aeruginosa PAK Pilin.” *Molecular Cell* 11 (5): 1139–50. https://doi.org/10.1016/S1097-2765(03)00170-9.

Craig, Lisa, Niels Volkmann, Andrew S. Arvai, et al. 2006. “Type IV Pilus Structure by Cryo-Electron Microscopy and Crystallography: Implications for Pilus Assembly and Functions.” *Molecular Cell* 23 (5): 651–62. https://doi.org/10.1016/j.molcel.2006.07.004.

Day, Michaela, Rachel Pitt, Nisha Mody, et al. 2022. “Detection of 10 Cases of Ceftriaxone-Resistant Neisseria Gonorrhoeae in the United Kingdom, December 2021 to June 2022.” *Euro Surveillance: Bulletin Europeen Sur Les Maladies Transmissibles = European Communicable Disease Bulletin* 27 (46). https://doi.org/10.2807/1560-7917.ES.2022.27.46.2200803.

Dees, John E., and J. a. C. Colston. 1937. “The Use of Sulfanilamide in Gonococcic Infections: Preliminary Report.” *Journal of the American Medical Association* 108 (22): 1855–58. https://doi.org/10.1001/jama.1937.02780220013003.

Denise, Rémi, Sophie S. Abby, and Eduardo P. C. Rocha. 2019. “Diversification of the Type IV Filament Superfamily into Machines for Adhesion, Protein Secretion, DNA Uptake, and Motility.” *PLoS Biology* 17 (7): e3000390. https://doi.org/10.1371/journal.pbio.3000390.

Ellison, Courtney K., Triana N. Dalia, Ankur B. Dalia, and Yves V. Brun. 2019. “Real-Time Microscopy and Physical Perturbation of Bacterial Pili Using Maleimide-Conjugated Molecules.” *Nature Protocols* 14 (6): 1803–19. https://doi.org/10.1038/s41596-019-0162-6.

Ellison, Courtney K., Triana N. Dalia, Alfredo Vidal Ceballos, et al. 2018. “Retraction of DNA-Bound Type IV Competence Pili Initiates DNA Uptake during Natural Transformation in Vibrio Cholerae.” *Nature Microbiology* 3 (7): 773–80. https://doi.org/10.1038/s41564-018-0174-y.

Ellison, Courtney K., Jingbo Kan, Jennifer L. Chlebek, et al. 2019. “A Bifunctional ATPase Drives Tad Pilus Extension and Retraction.” *Science Advances* 5 (12): eaay2591. https://doi.org/10.1126/sciadv.aay2591.

Ellison, Courtney K., Jingbo Kan, Rebecca S. Dillard, et al. 2017. “Obstruction of Pilus Retraction Stimulates Bacterial Surface Sensing.” *Science (New York, N.Y.)* 358 (6362): 535–38. https://doi.org/10.1126/science.aan5706.

Ellison, Courtney K., Gregory B. Whitfield, and Yves V. Brun. 2022. “Type IV Pili: Dynamic Bacterial Nanomachines.” *FEMS Microbiology Reviews* 46 (2): fuab053. https://doi.org/10.1093/femsre/fuab053.

Ellison, Taylor J., and Courtney K. Ellison. 2025. “Improved DNA Binding to a Type IV Minor Pilin Increases Natural Transformation.” *Nucleic Acids Research* 53 (10): gkaf467. https://doi.org/10.1093/nar/gkaf467.

Ellison, Taylor J., Ian Y. Yen, P. Lynne Howell, and Courtney K. Ellison. 2025. “FimX Regulates Type IV Pilus Localization via the Pil-Chp Chemosensory System in Acinetobacter Baylyi.” *Molecular Biology of the Cell* 36 (9): ar113. https://doi.org/10.1091/mbc.E25-05-0242.

Eyre, JohnW. H., and BernardH. Stewart. 1909. “THE TREATMENT OF GONOCOCCUS INFECTIONS BY VACCINES.” *The Lancet*, Originally published as Volume 2, Issue 4480, vol. 174 (4480): 76–81. https://doi.org/10.1016/S0140-6736(01)32510-2.

Fiore, Michael A., Jordan C. Raisman, Narayan H. Wong, André O. Hudson, and Crista B. Wadsworth. 2020. “Exploration of the Neisseria Resistome Reveals Resistance Mechanisms in Commensals That May Be Acquired by N. Gonorrhoeae through Horizontal Gene Transfer.” *Antibiotics (Basel, Switzerland)* 9 (10): E656. https://doi.org/10.3390/antibiotics9100656.

Francetic, Olivera, Nienke Buddelmeijer, Shawn Lewenza, Carol A. Kumamoto, and Anthony P. Pugsley. 2007. “Signal Recognition Particle-Dependent Inner Membrane Targeting of the PulG Pseudopilin Component of a Type II Secretion System.” *Journal of Bacteriology* 189 (5): 1783–93. https://doi.org/10.1128/JB.01230-06.

Gibson, Daniel G., Lei Young, Ray-Yuan Chuang, J. Craig Venter, Clyde A. Hutchison, and Hamilton O. Smith. 2009. “Enzymatic Assembly of DNA Molecules up to Several Hundred Kilobases.” *Nature Methods* 6 (5): 5. https://doi.org/10.1038/nmeth.1318.

Giltner, Carmen L., Ylan Nguyen, and Lori L. Burrows. 2012. “Type IV Pilin Proteins: Versatile Molecular Modules.” *Microbiology and Molecular Biology Reviews: MMBR* 76 (4): 740–72. https://doi.org/10.1128/MMBR.00035-12.

Gonzalez Rivera, Alba Katiria, and Katrina T. Forest. 2017. “Shearing and Enrichment of Extracellular Type IV Pili.” *Methods in Molecular Biology (Clifton, N.J.)* 1615: 311–20. https://doi.org/10.1007/978-1-4939-7033-9_25.

Grünwald, David, Shailesh M. Shenoy, Sean Burke, and Robert H. Singer. 2008. “Calibrating Excitation Light Fluxes for Quantitative Light Microscopy in Cell Biology.” *Nature Protocols* 3 (11): 1809–14. https://doi.org/10.1038/nprot.2008.180.

Gu, Yangqi, Vishok Srikanth, Aldo I. Salazar-Morales, et al. 2021. “Structure of Geobacter Pili Reveals Secretory Rather than Nanowire Behaviour.” *Nature* 597 (7876): 430–34. https://doi.org/10.1038/s41586-021-03857-w.

Guo, Shuaiqi, Yunjie Chang, Yves V. Brun, P. Lynne Howell, Lori L. Burrows, and Jun Liu. 2024. “PilY1 Regulates the Dynamic Architecture of the Type IV Pilus Machine in Pseudomonas Aeruginosa.” *Nature Communications* 15 (1): 9382. https://doi.org/10.1038/s41467-024-53638-y.

Haas, R., H. Schwarz, and T. F. Meyer. 1987. “Release of Soluble Pilin Antigen Coupled with Gene Conversion in Neisseria Gonorrhoeae.” *Proceedings of the National Academy of Sciences of the United States of America* 84 (24): 9079–83. https://doi.org/10.1073/pnas.84.24.9079.

Hazes, Bart, Parimi A. Sastry, Koto Hayakawa, Randy J. Read, and Randall T. Irvin. 2000. “Crystal Structure of *Pseudomonas Aeruginosa* PAK Pilin Suggests a Main-Chain-Dominated Mode of Receptor Binding1.” *Journal of Molecular Biology* 299 (4): 1005–17. https://doi.org/10.1006/jmbi.2000.3801.

Helaine, Sophie, David H. Dyer, Xavier Nassif, Vladimir Pelicic, and Katrina T. Forest. 2007. “3D Structure/Function Analysis of PilX Reveals How Minor Pilins Can Modulate the Virulence Properties of Type IV Pili.” *Proceedings of the National Academy of Sciences of the United States of America* 104 (40): 15888–93. https://doi.org/10.1073/pnas.0707581104.

Herrell, Wallace E., Edward N. Cook, and Luther Thompson. 1943. “Use of Penicillin in Sulfonamide Resistant Gonorrheal Infections.” *Journal of the American Medical Association* 122 (5): 289–92. https://doi.org/10.1001/jama.1943.02840220021005.

Hill, Stuart A., Thao L. Masters, and Jenny Wachter. 2016. “Gonorrhea - an Evolving Disease of the New Millennium.” *Microbial Cell (Graz, Austria)* 3 (9): 371–89. https://doi.org/10.15698/mic2016.09.524.

Hobbs, Marcia M., P. Frederick Sparling, Myron S. Cohen, William M. Shafer, Carolyn D. Deal, and Ann E. Jerse. 2011. “Experimental Gonococcal Infection in Male Volunteers: Cumulative Experience with Neisseria Gonorrhoeae Strains FA1090 and MS11mkC.” *Frontiers in Microbiology* 2: 123. https://doi.org/10.3389/fmicb.2011.00123.

Hu, Linda I., Elizabeth A. Stohl, and H. Steven Seifert. 2022. “The Neisseria Gonorrhoeae Type IV Pilus Promotes Resistance to Hydrogen Peroxide- and LL-37-Mediated Killing by

Modulating the Availability of Intracellular, Labile Iron." *PLOS Pathogens* 18 (6): e1010561. https://doi.org/10.1371/journal.ppat.1010561.

Hughes-Games, Alex, Sean A. Davis, and Darryl J. Hill. 2022. "Direct Visualization of Sequence-Specific DNA Binding by Gonococcal Type IV Pili." *Microbiology (Reading, England)* 168 (8). https://doi.org/10.1099/mic.0.001224.

Jarvis, Gary A., and Theresa L. Chang. 2012. "Modulation of HIV Transmission by Neisseria Gonorrhoeae: Molecular and Immunological Aspects." *Current HIV Research* 10 (3): 211–17. https://doi.org/10.2174/157016212800618138.

Jefferson, Amber, Amanda Smith, Pius S. Fasinu, and Dorothea K. Thompson. 2021. "Sexually Transmitted Neisseria Gonorrhoeae Infections—Update on Drug Treatment and Vaccine Development." *Medicines* 8 (2): 11. https://doi.org/10.3390/medicines8020011.

Jonsson, A. B., G. Nyberg, and S. Normark. 1991. "Phase Variation of Gonococcal Pili by Frameshift Mutation in pilC, a Novel Gene for Pilus Assembly." *The EMBO Journal* 10 (2): 477–88. https://doi.org/10.1002/j.1460-2075.1991.tb07970.x.

Jose, Predesh Parasseril, Vatsan Vivekanandan, and Kunjumani Sobhanakumari. 2020. "Gonorrhea: Historical Outlook." *Journal of Skin and Sexually Transmitted Diseases* 2 (2): 110–14. https://doi.org/10.25259/JSSTD_4_2020.

Karuppiah, Vijaykumar, Angela Thistlethwaite, and Jeremy P. Derrick. 2016. "Structures of Type IV Pilins from *Thermus Thermophilus* Demonstrate Similarities with Type II Secretion System Pseudopilins." *Journal of Structural Biology* 196 (3): 375–84. https://doi.org/10.1016/j.jsb.2016.08.006.

Kaushik, Sharbani, Haoze He, and Ross E. Dalbey. 2022. "Bacterial Signal Peptides- Navigating the Journey of Proteins." *Frontiers in Physiology* 13: 933153. https://doi.org/10.3389/fphys.2022.933153.

Kawahara, Kazuki, Hiroya Oki, Shunsuke Fukakusa, et al. 2016. "Homo-Trimeric Structure of the Type IVb Minor Pilin CofB Suggests Mechanism of CFA/III Pilus Assembly in Human Enterotoxigenic Escherichia Coli." *Journal of Molecular Biology* 428 (6): 1209–26. https://doi.org/10.1016/j.jmb.2016.02.003.

Kellogg, Douglas S., William L. Peacock, W. E. Deacon, L. Brown, and Carl I. Pirkle. 1963. "Neisseria Gonorrhoeae i. VIRULENCE GENETICALLY LINKED TO CLONAL VARIATION." *Journal of Bacteriology* 85 (6): 1274–79. https://doi.org/10.1128/jb.85.6.1274-1279.1963.

Koch, Matthias D., Matthew E. Black, Endao Han, Joshua W. Shaevitz, and Zemer Gitai. 2022. "Pseudomonas Aeruginosa Distinguishes Surfaces by Stiffness Using Retraction of Type IV Pili." *Proceedings of the National Academy of Sciences of the United States of America* 119 (20): e2119434119. https://doi.org/10.1073/pnas.2119434119.

Kollman, Justin M., Andreas Merdes, Lionel Mourey, and David A. Agard. 2011. “Microtubule Nucleation by γ-Tubulin Complexes.” *Nature Reviews. Molecular Cell Biology* 12 (11): 709–21. https://doi.org/10.1038/nrm3209.

Korotkov, Konstantin V., and Wim G. J. Hol. 2008. “Structure of the GspK-GspI-GspJ Complex from the Enterotoxigenic Escherichia Coli Type 2 Secretion System.” *Nature Structural & Molecular Biology* 15 (5): 462–68. https://doi.org/10.1038/nsmb.1426.

Korotkov, Konstantin V., and Maria Sandkvist. 2019. “Architecture, Function, and Substrates of the Type II Secretion System.” *EcoSal Plus* 8 (2). https://doi.org/10.1128/ecosalplus.ESP-0034-2018.

Korotkov, Konstantin V., Maria Sandkvist, and Wim G. J. Hol. 2012. “The Type II Secretion System: Biogenesis, Molecular Architecture and Mechanism.” *Nature Reviews. Microbiology* 10 (5): 336–51. https://doi.org/10.1038/nrmicro2762.

Kraus-Römer, Sebastian, Isabelle Wielert, Isabel Rathmann, Jan Grossbach, and Berenike Maier. 2022. “External Stresses Affect Gonococcal Type 4 Pilus Dynamics.” *Frontiers in Microbiology* 13: 839711. https://doi.org/10.3389/fmicb.2022.839711.

Lam, Anita Y., Els Pardon, Konstantin V. Korotkov, Wim G. J. Hol, and Jan Steyaert. 2009. “Nanobody-Aided Structure Determination of the EpsI:EpsJ Pseudopilin Heterodimer from Vibrio Vulnificus.” *Journal of Structural Biology* 166 (1): 8–15. https://doi.org/10.1016/j.jsb.2008.11.008.

Lam, Trinh, Courtney K. Ellison, David T. Eddington, Yves V. Brun, Ankur B. Dalia, and Donald A. Morrison. 2021. “Competence Pili in Streptococcus Pneumoniae Are Highly Dynamic Structures That Retract to Promote DNA Uptake.” *Molecular Microbiology* 116 (2): 381–96. https://doi.org/10.1111/mmi.14718.

Laurenceau, Raphaël, Gérard Péhau-Arnaudet, Sonia Baconnais, et al. 2013. “A Type IV Pilus Mediates DNA Binding during Natural Transformation in Streptococcus Pneumoniae.” *PLoS Pathogens* 9 (6): e1003473. https://doi.org/10.1371/journal.ppat.1003473.

Leduc, Isabelle, Kristie L. Connolly, Afrin Begum, et al. 2020. “The Serogroup B Meningococcal Outer Membrane Vesicle-Based Vaccine 4CMenB Induces Cross-Species Protection against Neisseria Gonorrhoeae.” *PLoS Pathogens* 16 (12): e1008602. https://doi.org/10.1371/journal.ppat.1008602.

Lee, Kachiu C., and Barry Ladizinski. 2012. “The Clap Heard Round the World.” *Archives of Dermatology* 148 (2): 223. https://doi.org/10.1001/archdermatol.2011.2716.

Lenz, Jonathan D., and Joseph P. Dillard. 2018. “Pathogenesis of Neisseria Gonorrhoeae and the Host Defense in Ascending Infections of Human Fallopian Tube.” *Frontiers in Immunology* 9: 2710. https://doi.org/10.3389/fimmu.2018.02710.

Maier, Berenike, Laura Potter, Magdalene So, Cynthia D. Long, Hank S. Seifert, and Michael P. Sheetz. 2002. “Single Pilus Motor Forces Exceed 100 pN.” *Proceedings of the National*

Academy of Sciences of the United States of America 99 (25): 16012–17. https://doi.org/10.1073/pnas.242523299.

Makarova, Kira S., Eugene V. Koonin, and Sonja-Verena Albers. 2016. "Diversity and Evolution of Type IV Pili Systems in Archaea." *Frontiers in Microbiology* 7 (May): 667. https://doi.org/10.3389/fmicb.2016.00667.

Marshall, Helen S., Prabha H. Andraweera, James Ward, et al. 2022. "An Observational Study to Assess the Effectiveness of 4CMenB against Meningococcal Disease and Carriage and Gonorrhea in Adolescents in the Northern Territory, Australia—Study Protocol." *Vaccines* 10 (2): 2. https://doi.org/10.3390/vaccines10020309.

McChesney, D., E. C. Tramont, J. W. Boslego, J. Ciak, J. Sadoff, and C. C. Brinton. 1982. "Genital Antibody Response to a Parenteral Gonococcal Pilus Vaccine." *Infection and Immunity* 36 (3): 1006–12. https://doi.org/10.1128/iai.36.3.1006-1012.1982.

Merz, A. J., M. So, and M. P. Sheetz. 2000. "Pilus Retraction Powers Bacterial Twitching Motility." *Nature* 407 (6800): 98–102. https://doi.org/10.1038/35024105.

Merz, Alexey J., and Katrina T. Forest. 2002. "Bacterial Surface Motility: Slime Trails, Grappling Hooks and Nozzles." *Current Biology: CB* 12 (8): R297-303. https://doi.org/10.1016/s0960-9822(02)00806-0.

Mirdita, Milot, Konstantin Schütze, Yoshitaka Moriwaki, Lim Heo, Sergey Ovchinnikov, and Martin Steinegger. 2022. "ColabFold: Making Protein Folding Accessible to All." *Nature Methods* 19 (6): 679–82. https://doi.org/10.1038/s41592-022-01488-1.

Mom, Jeremy, Iman Chouikha, Odile Valette, Laetitia Pieulle, and Vladimir Pelicic. 2024. "Systematic Functional Analysis of the Com Pilus in Streptococcus Sanguinis: A Minimalistic Type 4 Filament Dedicated to DNA Uptake in Monoderm Bacteria." *mBio* 15 (1): e0266723. https://doi.org/10.1128/mbio.02667-23.

Mom, Jérémy, Odile Valette, Laetitia Pieulle, and Vladimir Pelicic. 2025. "Unraveling the Molecular Mechanisms of DNA Capture by the Com Pilus in Naturally Transformable Monoderm Bacteria." *mBio* 16 (6): e0085125. https://doi.org/10.1128/mbio.00851-25.

Mullins, R. Dyche, John A. Heuser, and Thomas D. Pollard. 1998. "The Interaction of Arp2/3 Complex with Actin: Nucleation, High Affinity Pointed End Capping, and Formation of Branching Networks of Filaments." *Proceedings of the National Academy of Sciences of the United States of America* 95 (11): 6181–86. https://doi.org/10.1073/pnas.95.11.6181.

Nassif, X., J. L. Beretti, J. Lowy, et al. 1994. "Roles of Pilin and PilC in Adhesion of Neisseria Meningitidis to Human Epithelial and Endothelial Cells." *Proceedings of the National Academy of Sciences of the United States of America* 91 (9): 3769–73. https://doi.org/10.1073/pnas.91.9.3769.

Ng, Dixon, Tony Harn, Tuba Altindal, et al. 2016. “The Vibrio Cholerae Minor Pilin TcpB Initiates Assembly and Retraction of the Toxin-Coregulated Pilus.” *PLoS Pathogens* 12 (12): e1006109. https://doi.org/10.1371/journal.ppat.1006109.

Nguyen, Ylan, Seiji Sugiman-Marangos, Hanjeong Harvey, et al. 2015. “Pseudomonas Aeruginosa Minor Pilins Prime Type IVa Pilus Assembly and Promote Surface Display of the PilY1 Adhesin.” *The Journal of Biological Chemistry* 290 (1): 601–11. https://doi.org/10.1074/jbc.M114.616904.

Noori Goodarzi, Narjes, and Mohammad Reza Pourmand. 2026. “Innovations, Challenges, and Gaps in the Development of an Effective Vaccine against Neisseria Gonorrhoeae, a Narrative Review.” *Molecular Immunology* 189 (January): 13–30. https://doi.org/10.1016/j.molimm.2025.11.019.

Nunn, D. N., and S. Lory. 1991. “Product of the Pseudomonas Aeruginosa Gene pilD Is a Prepilin Leader Peptidase.” *Proceedings of the National Academy of Sciences of the United States of America* 88 (8): 3281–85. https://doi.org/10.1073/pnas.88.8.3281.

Obeid Charrouf, Farah, Gregory B. Whitfield, Courtney K. Ellison, and Yves V. Brun. 2025. “Stimulation of the Caulobacter Crescentus Surface Sensing Pathway by Deletion of a Specialized Minor Pilin-like Gene.” *mBio* 16 (11): e0230225. https://doi.org/10.1128/mbio.02302-25.

Orans, Jillian, Michael D. L. Johnson, Kimberly A. Coggan, et al. 2010. “Crystal Structure Analysis Reveals Pseudomonas PilY1 as an Essential Calcium-Dependent Regulator of Bacterial Surface Motility.” *Proceedings of the National Academy of Sciences* 107 (3): 1065–70. https://doi.org/10.1073/pnas.0911616107.

Páez-Pérez, Edgar D., Araceli Hernández-Sánchez, Elvia Alfaro-Saldaña, and J. Viridiana García-Meza. 2025. “Simplified Method for Purifying Full-Length Major Type IV Pilins: PilA from Acidithiobacillus Thiooxidans.” *MethodsX* 15 (December): 103520. https://doi.org/10.1016/j.mex.2025.103520.

Parge, H. E., S. L. Bernstein, C. D. Deal, et al. 1990. “Biochemical Purification and Crystallographic Characterization of the Fiber-Forming Protein Pilin from Neisseria Gonorrhoeae.” *The Journal of Biological Chemistry* 265 (4): 2278–85.

Punsalang, A. P., and W. D. Sawyer. 1973. “Role of Pili in the Virulence of Neisseria Gonorrhoeae.” *Infection and Immunity* 8 (2): 255–63. https://doi.org/10.1128/iai.8.2.255-263.1973.

Quillin, Sarah Jane, and H. Steven Seifert. 2018. “Neisseria Gonorrhoeae Host Adaptation and Pathogenesis.” *Nature Reviews. Microbiology* 16 (4): 226–40. https://doi.org/10.1038/nrmicro.2017.169.

Ramboarina, Stéphanie, Paula Fernandes, Peter Simpson, Gad Frankel, Michael Donnenberg, and Stephen Matthews. 2004. “Complete Resonance Assignments of Bundlin (BfpA) from the Bundle-Forming Pilus of Enteropathogenic Escherichia Coli.” *Journal of*

Biomolecular NMR 29 (3): 427–28. https://doi.org/10.1023/B:JNMR.0000032511.89525.64.

Rotty, Jeremy D., Congying Wu, and James E. Bear. 2013. "New Insights into the Regulation and Cellular Functions of the ARP2/3 Complex." *Nature Reviews. Molecular Cell Biology* 14 (1): 7–12. https://doi.org/10.1038/nrm3492.

Sacharok, Alexandra L., Eric A. Porsch, Taylor A. Yount, Orlaith Keenan, and Joseph W. St Geme. 2022. "Kingella Kingae PilC1 and PilC2 Are Adhesive Multifunctional Proteins That Promote Bacterial Adherence, Twitching Motility, DNA Transformation, and Pilus Biogenesis." *PLoS Pathogens* 18 (3): e1010440. https://doi.org/10.1371/journal.ppat.1010440.

Sancta St. Cyr, M. D., M. D. Lindley Barbee, M. D. Kimberly A. Workowski, et al. 2020. "Update to CDC's Treatment Guidelines for Gonococcal Infection, 2020." *MMWR. Morbidity and Mortality Weekly Report* 69. https://doi.org/10.15585/mmwr.mm6950a6.

Sanger, WW. 1910. *The History of Prostitution*. Harper and Brothers.

Schmidt, K. A., H. Schneider, J. A. Lindstrom, et al. 2001. "Experimental Gonococcal Urethritis and Reinfection with Homologous Gonococci in Male Volunteers." *Sexually Transmitted Diseases* 28 (10): 555–64. https://doi.org/10.1097/00007435-200110000-00001.

Seifert, H. S., C. J. Wright, A. E. Jerse, M. S. Cohen, and J. G. Cannon. 1994. "Multiple Gonococcal Pilin Antigenic Variants Are Produced during Experimental Human Infections." *The Journal of Clinical Investigation* 93 (6): 2744–49. https://doi.org/10.1172/JCI117290.

Sheffield, Peter, Sarah Garrard, and Zygmunt Derewenda. 1999. "Overcoming Expression and Purification Problems of RhoGDI Using a Family of 'Parallel' Expression Vectors." *Protein Expression and Purification* 15 (1): 34–39. https://doi.org/10.1006/prep.1998.1003.

Singh, Pradip Kumar, Janay Little, and Michael S. Donnenberg. 2022. "Landmark Discoveries and Recent Advances in Type IV Pilus Research." *Microbiology and Molecular Biology Reviews: MMBR* 86 (3): e0007622. https://doi.org/10.1128/mmbr.00076-22.

Skerker, J. M., and H. C. Berg. 2001. "Direct Observation of Extension and Retraction of Type IV Pili." *Proceedings of the National Academy of Sciences of the United States of America* 98 (12): 6901–4. https://doi.org/10.1073/pnas.121171698.

Stern, A., M. Brown, P. Nickel, and T. F. Meyer. 1986. "Opacity Genes in Neisseria Gonorrhoeae: Control of Phase and Antigenic Variation." *Cell* 47 (1): 61–71. https://doi.org/10.1016/0092-8674(86)90366-1.

Studier, F. William. 2005. "Protein Production by Auto-Induction in High-Density Shaking Cultures." *Protein Expression and Purification* 41 (1): 207–34. https://doi.org/10.1016/j.pep.2005.01.016.

Sztanko, Kristina M., Taylor J. Ellison, Jill Greenlaw, et al. 2026. “A Prophage-Expressed Type IV Pilus Component Provides Anti-Phage Defense.” *Cell Reports* 45 (1): 116759. https://doi.org/10.1016/j.celrep.2025.116759.

Teufel, Felix, José Juan Almagro Armenteros, Alexander Rosenberg Johansen, et al. 2022. “SignalP 6.0 Predicts All Five Types of Signal Peptides Using Protein Language Models.” *Nature Biotechnology* 40 (7): 1023–25. https://doi.org/10.1038/s41587-021-01156-3.

Treuner-Lange, Anke, Yi-Wei Chang, Timo Glatter, et al. 2020. “PilY1 and Minor Pilins Form a Complex Priming the Type IVa Pilus in Myxococcus Xanthus.” *Nature Communications* 11 (1): 5054. https://doi.org/10.1038/s41467-020-18803-z.

Unemo, Magnus, H. Steven Seifert, Edward W. Hook, Sarah Hawkes, Francis Ndowa, and Jo-Anne R. Dillon. 2019. “Gonorrhoea.” *Nature Reviews Disease Primers* 5 (1): 79. https://doi.org/10.1038/s41572-019-0128-6.

Welker, Anton, Tom Cronenberg, Robert Zöllner, et al. 2018. “Molecular Motors Govern Liquidlike Ordering and Fusion Dynamics of Bacterial Colonies.” *Physical Review Letters* 121 (11): 118102. https://doi.org/10.1103/PhysRevLett.121.118102.

Whitchurch, C. B., M. Hobbs, S. P. Livingston, V. Krishnapillai, and J. S. Mattick. 1991. “Characterisation of a Pseudomonas Aeruginosa Twitching Motility Gene and Evidence for a Specialised Protein Export System Widespread in Eubacteria.” *Gene* 101 (1): 33–44. https://doi.org/10.1016/0378-1119(91)90221-v.

Winther-Larsen, H. C., F. T. Hegge, M. Wolfgang, S. F. Hayes, J. P. van Putten, and M. Koomey. 2001. “Neisseria Gonorrhoeae PilV, a Type IV Pilus-Associated Protein Essential to Human Epithelial Cell Adherence.” *Proceedings of the National Academy of Sciences of the United States of America* 98 (26): 15276–81. https://doi.org/10.1073/pnas.261574998.

Winther-Larsen, Hanne C., Matthew Wolfgang, Steven Dunham, et al. 2005. “A Conserved Set of Pilin-like Molecules Controls Type IV Pilus Dynamics and Organelle-Associated Functions in Neisseria Gonorrhoeae.” *Molecular Microbiology* 56 (4): 903–17. https://doi.org/10.1111/j.1365-2958.2005.04591.x.

Wolfgang, Matthew, Hae-Sun Park, Stanley F. Hayes, Jos P. M. van Putten, and Michael Koomey. 1998. “Suppression of an Absolute Defect in Type IV Pilus Biogenesis by Loss-of-Function Mutations in pilT, a Twitching Motility Gene in Neisseria Gonorrhoeae.” Biological Sciences. *Proceedings of the National Academy of Sciences* 95 (25): 14973–78.

World Health Organization, ed. 2024. *Updated Recommendations for the Treatment of Neisseria Gonorrhoeae, Chlamydia Trachomatis and Treponema Pallidum (Syphilis), and New Recommendations on Syphilis Testing and Partner Services*. World Health Organization.

Yanez, Marissa E., Konstantin V. Korotkov, Jan Abendroth, and Wim G. J. Hol. 2008. “Structure of the Minor Pseudopilin EpsH from the Type 2 Secretion System of Vibrio Cholerae.”

Journal of Molecular Biology 377 (1): 91–103. https://doi.org/10.1016/j.jmb.2007.08.041.

Zhang, Yichen, Frédérick Faucher, Wenwen Zhang, et al. 2018. "Structure-Guided Disruption of the Pseudopilus Tip Complex Inhibits the Type II Secretion in Pseudomonas Aeruginosa." *PLOS Pathogens* 14 (10): e1007343. https://doi.org/10.1371/journal.ppat.1007343.

Zuke, Jason D., Rachel Erickson, Katherine R. Hummels, and Briana M. Burton. 2023. "Visualizing Dynamic Competence Pili and DNA Capture throughout the Long Axis of Bacillus Subtilis." *Journal of Bacteriology* 205 (9): e0015623. https://doi.org/10.1128/jb.00156-23.

VITA

Justin N. Applegate grew up in the one stoplight town of LaFayette, New York. Their interest in science began at a young age thanks to their grandfather who was a retired science teacher. Justin's research career began as a high school intern at the biotechnology start-up Ichor Life Science. They graduated from SUNY Binghamton with a B.S. in Biochemistry. While studying at Binghamton they joined the lab of Dr. Eriks Rozners they were mentored by Dr. James A. MacKay. While in the Rozners lab they worked on creating sequence selective tools for the recognition of double-stranded non-coding RNA via triplex forming PNA. During the summer before their senior year, Justin was given the opportunity to work in Dana Miller's lab at the University of Washington studying the effect of arsenic exposure on SUMO nuclear localization in SUMO::GFP *C. elegans*. After graduating from Binghamton in 2020, Justin decided to return to Seattle and began their graduate studies at the University of Washington in the Department of Biochemistry. They joined the lab of Dr. Alexey Merz studying the tip located proteins that make up the type IV pilus of *N. gonorrhoeae.* They were awarded a predoctoral fellowship in the University of Washington STD/AIDS Research Training Program. During their PhD, they became involved in their union UAW local 4121, where they were elected a head steward representing the academic student employees of UW. While not in lab, Justin enjoys making music, foraging for mushrooms, and watching movies with friends.